

DUPLICATE ALSO



Met O (APR) Turbulence and Diffusion Note No. 217

**NAME II: A Scientific Overview**

by

**D.B. Ryall, R.H. Maryon & K.P. Kitchen**

**July 1995**

Met O (APR) (Atmospheric Processes Research)  
Meteorological Office  
London Road  
Bracknell  
Berkshire, RG12 2SZ

**Note:**

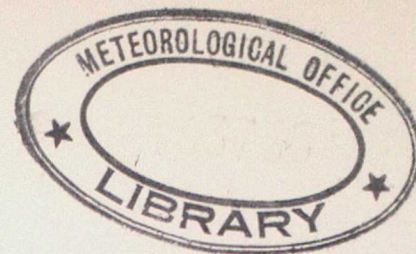
This paper has not been published. Permission to quote from it should be obtained from the Head, Atmospheric Processes Research, Met O(APR), Meteorological Office, London Road, Bracknell, Berkshire, RG12 2SZ.

ORGS UKMO T

Crown copyright 1995

**National Meteorological Library**  
FitzRoy Road, Exeter, Devon. EX1 3PB





# NAME II - A SCIENTIFIC OVERVIEW (Version 2\*)

D B Ryall, R H Maryon & K P Kitchen

July 1995

## SUMMARY

The UK Meteorological Office's operational Nuclear Accident Model (NAME) is used to simulate the medium and long range transport of hazardous airborne pollutants such as accidentally released radionuclides. The model provides estimates of air concentrations and dosages, together with estimates of the deposition of pollutants to the ground. It has direct telecommunications links with the Government's Department of Environment office which would become the Technical Coordination Centre controlling the national response to a nuclear emergency.

Under contract to the Ministry of Agriculture, Fisheries and Food and the Department of Environment the model has been upgraded and improved. In particular, a nested mesoscale facility has been added, providing much improved resolution over the UK. To maximise the benefit of this enhanced resolution, a new near-source diffusion scheme has been introduced. Other additions include improvements to the wet and dry deposition parametrizations, the introduction of a simple scheme to represent vertical mixing due to convection, and improved output capabilities. This report describes the current model (referred to as NAME II), its capabilities, and the basis of its underlying physics.

\* Note that this version replaces version 1, issued as a preliminary report in January 1995 with a limited distribution



3 8078 0003 0124 4



## Table of Contents

<b>1. INTRODUCTION.....</b>	<b>2</b>
<b>2. METEOROLOGICAL DATA .....</b>	<b>2</b>
2.1 Availability.....	3
2.2 Nested Structure.....	3
2.3 High Resolution Data.....	3
2.4 Derived Fields.....	3
2.5 Output Grids.....	5
<b>3. OVERALL MODEL STRUCTURE .....</b>	<b>5</b>
3.1 Code Structure.....	5
<b>4. RELEASE .....</b>	<b>6</b>
4.1 Source Definitions.....	6
4.2 Area Sources .....	7
4.3 Implementation .....	7
<b>5. ADVECTION AND DISPERSION .....</b>	<b>7</b>
5.1 Introduction.....	7
5.2 Meteorological Data .....	7
5.3 Random Walk Technique .....	8
5.4 Turbulence profiles .....	12
5.5 Boundary Conditions .....	15
5.6 Plume Rise.....	16
5.7 Implementation .....	18
5.8 Poles.....	18
5.9 Mixing by Convection.....	18
<b>6. LOSS PROCESSES .....</b>	<b>19</b>
6.1 Introduction.....	19
6.2 Wet Deposition.....	19
6.3 Dry Deposition .....	21
6.4 Turbulent Deposition .....	24
6.5 Radioactive Decay .....	24
<b>7. AUTOMATIC ADJUSTMENTS TO MODEL PRODUCTS .....</b>	<b>24</b>
7.1 Plume spread .....	25
7.2 Source reconstitution .....	25
7.3 Implementation .....	26
<b>8. OUTPUT .....</b>	<b>26</b>
8.1 Fields .....	26
8.2 Time series.....	27
8.3 Profiles .....	27
8.4 Graphics .....	27
<b>9. PLANNED MODEL IMPROVEMENTS .....</b>	<b>28</b>
9.1 Platform.....	28
9.2 Meteorological data .....	28
9.3 Advection and dispersion .....	28
9.4 Deposition .....	28
<b>10. REFERENCES.....</b>	<b>35</b>



# NAME II - A SCIENTIFIC OVERVIEW

D B Ryall, R H Maryon & K P Kitchen

UK Meteorological Office

## 1. INTRODUCTION

The UK Meteorological Office is a WMO Regional Specialist Met Centre (RSMC) with responsibility for providing forecasts of the transport of accidentally released radionuclides or other hazardous substances. The Nuclear Accident Response Model 'NAME' is used to simulate the transport and dispersion of airborne pollutants over medium and long ranges (>30 km). The model provides estimates of both instantaneous and time-integrated air concentrations of pollutant together with estimates of the deposition of pollutants to the ground by both wet and dry deposition processes. It has direct telecommunications links with the Government's Department of Environment office which would become the Technical Coordination Centre controlling the national response to a nuclear emergency.

The model is of a Lagrangian, Monte Carlo type in which emissions are modelled by releasing large numbers of 'particles' into the 'model atmosphere'. The particles are carried along passively by the ambient three-dimensional wind flow, with turbulent dispersion simulated by random walk techniques. Each particle represents a mass of released pollutant, which is reduced over time by both wet and dry deposition processes and radioactive decay. The model also has a 'radiological adjustment' package for modifying the plume spread and estimating source strengths from observational data.

This note gives an description of the model and its underlying physics. Details of the coding structure and user instructions can be found in the program documentation (Kitchen et al 1995) and the user guide (Maryon et al 1995), and further background information can be found in the previous model documentation (Maryon et al 1991).

## 2. METEOROLOGICAL DATA

Meteorological data are obtained from the global, regional and mesoscale versions of the UK Meteorological Office's numerical weather prediction (NWP) model, the Unified Model. These provide forecast data up to 144, 48 and 30 hours respectively at time intervals of 6, 3 and 1 hours, and horizontal resolutions of approximately 90, 50 and 16 km.

The vertical coordinate of the unified model is the hybrid  $\eta$  (eta) coordinate which is related to pressure,  $p$ , by

$$\eta = \frac{p}{p_*} + A \left( 1 - \frac{p_0}{p_*} \right)$$



where  $p_*$  is the surface pressure,  $p_0$  is a reference pressure taken as  $10^5$  Pa, and  $A$  is a function of height. Near the surface  $A=0$  so that the coordinate system follows the surface, then  $A$  varies with height until  $A=\eta$  near the 'top' of the atmosphere, resulting in  $\eta$  following pressure levels. The global, regional and mesoscale unified models have 20, 20 and 30  $\eta$  levels respectively; of which the NAME model currently uses 11, 11 and 24 levels. Figures 1-3 show the areas covered by the global, regional and mesoscale grids, together with their topography. A listing of the meteorological fields used is given in Table 1, and details of the vertical model levels used in Table 2.

## 2.1 Availability

Forecast data for each of the model versions is held on-line, together with archives of recent data (approximately 14, 8 and 5 days for the global, regional and mesoscale archives respectively). Model simulations can span both analysis and forecast periods.

## 2.2 Nested Structure

The model has a 'nested' structure, whereby the meteorology used to advect and apply depositions to each particle is taken from the highest resolution data available for that location and time (to avoid boundary problems the outer 5 grid points on the mesoscale and regional grids are not used). Thus a plume originating in the mesoscale area would be analysed at mesoscale resolution within the mesoscale model area, with material passing out of the area being analysed using lower resolution regional data (a plume may likewise spread into the higher resolution grid from a lower resolution grid). Similarly, for long period forecasts the plume in the mesoscale area would be analysed using high resolution mesoscale data up to the end of the forecast period, after which the plume would be analysed using lower resolution regional or global data for which longer forecasts are available. The model, therefore, has a global capability, but with the benefit of being able to resolve plume development and resultant deposition to higher resolutions when and where higher resolution meteorological data are available.

## 2.3 High Resolution Data

In addition to the unified model precipitation products, a high resolution (6 km) map of precipitation rates is available at hourly intervals. Precipitation rates are determined from the UK radar network (processed FRONTIERS images are used), the European radar network, satellite data, and mesoscale and regional NWP model output—it is used only in hindcast mode. Note that the high resolution data contains only total precipitation rates, and contains no information about precipitation type (i.e. convective or dynamic). The high resolution grid is also nested within the model, for use whenever and wherever it is requested and data are available. Figure 4 shows the areal coverage of the high resolution rainfall data.

## 2.4 Derived Fields

A number of derived fields are calculated from the unified model met fields; these include heights and boundary layer thicknesses at the model grid points.



#### 2.4.1 Model Level Heights

To readily convert from  $\eta$  coordinates to height above ground (in metres), a three dimensional field of heights is generated. The thickness  $\Delta z$  of each model layer is determined from

$$\Delta z = \frac{RT}{g} \log \left( \frac{p_1}{p_2} \right)$$

where  $p_1$  and  $p_2$  are the upper and lower pressure levels of the slab, and  $\bar{T}$  the mean temperature of the slab. Pressures are determined from

$$p = Ap_0 + p_*(\eta - A).$$

#### 2.4.2 Boundary Layer Depths

The correct determination of boundary layer depth is crucial for modelling the dispersion of airborne pollutants and the resultant deposition to the ground. For example, turbulent diffusion is significantly enhanced in the boundary layer, and only material in the boundary layer is subject to dry deposition. In NAME, fields of boundary layer depths are calculated on the temperature grid from wind and temperature profiles, using either a Richardson number or parcel technique.

##### 2.4.2.1 Richardson Number Technique

The presence of turbulent motion is inferred from the value of the gradient Richardson Number,  $R_i$ , which is calculated for a given model layer from

$$R_i = \frac{g \Delta\theta / \Delta z}{\bar{T} (\Delta u / \Delta z)^2}$$

where  $\Delta\theta / \Delta z$  and  $\Delta u / \Delta z$  are gradients of potential temperature and wind speed,  $g$  is the acceleration due to gravity and  $\bar{T}$  is the mean temperature of the layer. This is calculated for each model 'slab' (bounded by model levels) until the Richardson number exceeds a critical value,  $R_{ic}$ , taken as 1.3. The boundary layer top (in  $\eta$ ) is then taken as the bottom of the slab for which  $R_{ic}$  is exceeded.

Boundary layer depths are calculated at temperature grid points, but as the wind and temperature grids are staggered, wind values are first bilinearly interpolated to temperature grid points.

##### 2.4.2.2 Parcel Method

In the parcel method the dry adiabatic lapse rate (DALR) is followed from the surface (more strictly 1.5m) temperature, and the height at which it intersects the model environment curve (as defined by the model temperature profile) determined. Before following the DALR 1.2 °C is added to the 1.5m temperature unless this is below the temperature at the first model level above the surface (level 1 for the regional and



global grids, level 2 for the mesoscale, Tables 2a-2c), in which case 0.5 °C is added. The rationale for the technique is described in Maryon & Best (1992).

#### **2.4.2.3 Implementation**

The boundary layer depth is taken as the maximum of the Richardson Number and parcel method values. This generally results in the Richardson Number method being used in stable conditions and the parcel method in unstable conditions. A minimum boundary layer depth of 80 m ( $\eta=0.99$ ) is used, and a maximum boundary layer top of  $\eta=0.55$  (approx. 5000 m).

### **2.5 Output Grids**

For convenience and easy comparison diagnostic fields such as air concentrations, dosages and depositions are generated on the unified model grids (the centre of each analysis cell being defined by the NWP 'temperature' grid points). In addition diagnostic fields can be output on a latitude/longitude grid of user-defined size, origin and resolution. Air concentrations are determined over 10 levels in the vertical, as defined in Table 3, for all output grids. Wet depositions can also be diagnosed on the high resolution rainfall grid. Available diagnostic fields are listed in Table 4.

## **3. OVERALL MODEL STRUCTURE**

The model is currently implemented in FORTRAN 77 and is run on the UK Meteorological Office's mainframe Hitachi computer. Either a VAX or UNIX workstation running PV-WAVE can be used for subsequent data analysis and graphical display.

### **3.1 Code Structure**

This section briefly outlines the key elements of the structure of the model, which is also illustrated in Figure 6.

#### **Update/Newrun**

The model can be run in two modes: (i) 'newrun' for new releases; and (ii) 'update' for continuing simulations from previous simulations, i.e. the simulation is started from the final particle positions, masses and deposition fields calculated during a previous simulation. Using update it is possible to perform dispersion calculations covering periods longer than the on-line archives.

#### **Main Loop**

The main loop is based on a user-definable timestep, typically 300, 600 or 900 seconds. The main elements of the loop include:

- (i) loading met data for each requested grid if available (fields are available at 6, 3 & 1 hour intervals for the global, regional, mesoscale grids respectively). Fields



are loaded for two consecutive data times to allow interpolation of met data in time;

- (ii) calculating met fields such as boundary layer depths and heights;
- (iii) releasing particles from all active sources;
- (iv) assigning particles to the highest resolution grid available at that time and place: if all grids are being used then mesoscale particles are defined as those within the mesoscale area, regional particles as those within the regional area but outside the mesoscale area, and global particles those neither within the mesoscale or regional areas.
- (v) advecting particles and perturbing their positions to represent diffusion (the diffusion scheme may require shorter timesteps---Section 5);
- (vi) applying radioactive decay to all particles and deposition fields;
- (vii) depleting particle masses due to wet and dry deposition;
- (viii) applying particle mass loss/gain due to chemistry;
- (ix) managing particle numbers - to help prevent excessive numbers of particles options exist to lose particles if they leave a user-defined area, or if their mass falls below a user-defined value;
- (x) updating diagnostic fields on all requested output grids (e.g. deposition fields, air concentrations and dosages);
- (xi) outputting diagnostic if and when requested (fields, profiles and timeseries);
- (xii) particle splitting - an option exists to maintain a given minimum density of particles per grid square. If the number of particles in a grid cell falls below a user-defined value, each of the particles in that grid cell are split into two new particles, each carrying half of the mass of pollutant. This ensures that sufficient particles are used to represent the plume, whatever its history. Constraints are applied to prevent too many new particles being generated.

## 4. RELEASE

In the NAME model the pollutant is represented by large numbers of particles 'released' into the model atmosphere. Each particle can represent the mass or activity of a number of pollutant species. In what follows 'mass' represents either mass or radioactive activity.

### 4.1 Source Definitions

A number of sources can be defined for each model run. Each source is characterised by its release rate for each species as a function of both time and height ( $\eta$ ). Several time 'windows' can be defined (by a start and end time: e.g. 0 to 6 hours), each with a



given release rate for each species. Similarly the vertical release profile is defined for each time 'window' by a number of vertical 'slabs' (e.g.  $\eta=1.0$  to  $0.9$ ), each representing a fraction of the total release rate. Note that zero thickness slabs can be defined for releases from fixed heights, and zero length time windows can be defined for puff releases. With this approach complex release profiles can be readily specified.

## 4.2 Area Sources

Each source can be defined as a point or rectangular area source. An area source is defined by its length in metres in the x (east-west) and y (north-south) directions. Each particle released from an area source is given an initial x,y coordinate randomly chosen from within the area. Simple line sources aligned north-south or east-west can be defined simply by adopting a zero length in the appropriate direction.

## 4.3 Implementation

Each timestep all sources are checked to determine whether a release is required for the current time. For each 'live' source identified particles are released from each defined vertical slab, with the vertical coordinate being chosen randomly from within the slab. The time of release is also chosen at random within the timestep (or within the release time 'window' if shorter). The number of particles released is  $N=P\Delta tV_f$ , where  $P$  is the particle release rate,  $\Delta t$  is the current timestep and  $V_f$  is the fraction of material to be released from a given slab. Alternatively, the number of particles released can be based on a user-defined particle mass, i.e.  $N=R\Delta tV_f/M$  where  $R$  is the mass release rate and  $M$  is the user-defined particle mass. A minimum of one particle is released per 'live' vertical slab and timestep.

# 5. ADVECTION AND DISPERSION

## 5.1 Introduction

Particles are advected in three dimensions by model winds, with turbulent dispersion simulated by random walk techniques which take into account the turbulent velocity structure of the atmospheric boundary layer. The random velocity components are based on vertical profiles of the vertical velocity variances and Lagrangian timescales, which are mostly derived from published empirical fits to observational data. Separate formulae are used for stable and unstable conditions. For unstable conditions both Gaussian and non-Gaussian (skewed) turbulence schemes are available.

## 5.2 Meteorological Data

All meteorological data are linearly interpolated in space (either 2D or 3D depending on data type) to particle positions, and in time to the start of the current model step.



### 5.3 Random Walk Technique

The description of the random walk technique is summarised from Physick & Maryon (1995), although later revisions have been incorporated.

Particles are advected each timestep using

$$\mathbf{x}_{t+\Delta t} = \mathbf{x}_t + [\mathbf{u}(\mathbf{x}_t) + \mathbf{u}'(\mathbf{x}_t)]\Delta t \quad (5.1)$$

where  $\mathbf{x}(x,y,\eta)$  are the particle position vectors,  $\mathbf{u}(x,y,\eta)$  and  $\mathbf{u}'(x,y,\eta)$  the wind velocity and turbulent velocity vectors, and  $\Delta t$  is the timestep.

The subgrid velocities are obtained from a differential equation, first proposed by Langevin in 1908 as a model for Brownian motion. Although a general form of the Langevin equation exists which is valid for non-stationary, non-Gaussian (skewed) and inhomogeneous turbulence (Thomson, 1987), simpler forms of this equation can be applied when the turbulence is assumed to be Gaussian or homogeneous. By skewed it is meant that the probability that a sampled vertical velocity will be positive is not the same as that it will be negative; in Gaussian turbulence the probabilities are equal. An example of the former is convective turbulence, where downdrafts occupy a greater area than updrafts and are in general weaker. By inhomogeneous, we mean varying in vertical (turbulence is assumed homogeneous in the horizontal). In the next sections we present the different forms of the Langevin equation used in the model according to the type of turbulence being parametrized.

#### 5.3.1 Horizontal Motion

Assuming that the components of the turbulent motions are uncorrelated, the turbulent velocity component in the  $x$  direction is obtained from the differential equation

$$du' = adt + bd\xi \quad (5.2)$$

where the first term on the right hand side represents a 'memory' of previous motion and the second term an innovation. The coefficients  $a$  and  $b$  are defined by

$$a = -\frac{u'}{\tau_x}$$

$$b = \left( \frac{2\sigma_u^2}{\tau_x} \right)^{0.5}$$

where  $\tau_x$  is the Lagrangian timescale for the  $x$  component of the turbulence and  $\sigma_u^2$  the horizontal velocity variance. The  $d\xi$  are increments of a random process; they are here taken as Gaussian with mean zero and variance  $dt$ . Thus the turbulent velocity component can be expressed as



$$u'_{t+\Delta t} = u'_t \left(1 - \frac{\Delta t}{\tau_x}\right) + \left(\frac{2\sigma_u^2 \Delta t}{\tau_x}\right)^{1/2} r_t \quad (5.3)$$

where  $r_t$  is a random Gaussian variable of zero mean and unit variance. The expression for the  $v$  component is similar.

### 5.3.2 Vertical Motion

#### 5.3.2.1 Gaussian Turbulence

Whilst this formulation is adequate for the  $u$  and  $v$  components, where changes in the horizontal are small, the situation in the vertical is more complex as  $\sigma_w$  is not constant with height, resulting in particles tending to collect at levels of small  $\sigma_w$ . To account for this we use:

$$w'_{t+\Delta t} = w'_t \left(1 - \frac{\Delta t}{\tau_w}\right) + \left(\frac{2\sigma_w^2 \Delta t}{\tau_w}\right)^{1/2} r_t + \frac{\Delta t}{\sigma_w} \frac{\partial \sigma_w}{\partial z} (\sigma_w^2 + w'^2) \quad (5.4)$$

which is equivalent to the Wilson-Thompson (1983) model described in Physick & Maryon (1995). The final term on the right represents a 'drift' velocity', which prevents particles collecting in regions of low  $\sigma_w$ .

#### 5.3.2.2 Skewed Turbulence

Under one option the turbulence profile in the convectively unstable boundary layer can be assumed non-Gaussian (i.e. skewed). Once again, the general form of the Langevin Equation (5.2) is used, but the drift and diffusion coefficients  $a$  and  $b$  are specified differently. The corresponding equation to (5.2) is

$$dw' = a dt + b d\xi \quad (5.5)$$

where  $b = (C_0 \varepsilon)^{1/2}$ ,  $\varepsilon$  is the rate of dissipation of turbulent kinetic energy and  $C_0$  is a universal constant. Uncertainty surrounds the value of  $C_0$ , although 2.0 is usually used for unstable conditions. The Lagrangian timescale  $\tau_w$  can be related to  $\varepsilon$  by the relation

$$\tau_w = \frac{2\sigma_w^2}{C_0 \varepsilon}$$

The coefficient  $a$  is a function of  $\sigma_w$  and  $\varepsilon$ , both measurable quantities, rather than  $\tau_w$  which is only clearly defined when the turbulence is homogeneous and stationary. Note too that it is not necessary to incorporate the skewness  $Sk$  of the convective boundary layer in the diffusive (random) term, which remains Gaussian. Thus the finite-difference form of Equation 5.5 is

$$w'_{t+\Delta t} = w'_t + a \Delta t + (C_0 \varepsilon \Delta t)^{1/2} r_t$$



An expression for the function  $a$  is obtained by solving the following form of the Fokker-Planck equation (Thomson, 1987),

$$\frac{\partial(aP_E)}{\partial w} = -\frac{\partial P_E}{\partial t} - \frac{\partial(wP_E)}{\partial z} + \frac{1}{2}C_0\varepsilon \frac{\partial^2 P_E}{\partial w^2} \quad (5.7)$$

subject to the boundary condition  $aP_E \rightarrow 0$  as  $|w'| \rightarrow \infty$ .  $P_E$  is the probability density function (PDF) made up of two Gaussian functions, one representing the updrafts (+) and the other representing the downdrafts (-) of the convective boundary layer, and written as

$$P_E = pN(m_+, \sigma_+) + (1-p)N(m_-, \sigma_-)$$

with

$$N(m, \sigma) = \frac{(2\pi)^{-0.5}}{\sigma} \exp\left(-\frac{(w' - m)^2}{2\sigma^2}\right)$$

Here  $p$  is the probability of a particle being in an updraft,  $m_+$  is the mean velocity in an updraft and  $\sigma_+$  is the velocity standard deviation in an updraft, and similarly  $m_-$ ,  $\sigma_-$  for the downdraft terms. The first three moments of  $P_E$  are equated to the first three moments of the vertical velocity distribution ( $0, \sigma_w^2$  and  $S_w^3$  respectively, where  $S_w^3 = Sk \sigma_w^3$ ) and the resulting equations are solved for the variables  $p$ ,  $m_+$  and  $m_-$ , by making the assumption  $\sigma = |m|$  for both updrafts and downdrafts (see for example Hudson and Thomson, 1994). The solutions are

$$p = 0.5 \left( 1 - \left( \frac{Sk^2}{8 + Sk^2} \right)^{0.5} \right) \quad (5.8)$$

$$m_+^2 = \frac{0.5\sigma_w^2(1-p)}{p} \quad (5.9)$$

$$m_- = -\frac{m_+p}{1-p} \quad (5.10)$$

where  $Sk = (S_w/\sigma_w)^3$  is the degree of skewness of the turbulence.

By means of a little calculus, the solution of Equation 5.7 can be shown to be (see for example Luhar and Britter, 1989)

$$a = \frac{\phi_+ + \phi_-}{P_E} \quad (5.11)$$

where



$$\phi_+ = -\frac{1}{2}C_0 \varepsilon p N_+ (w' - m_+) / \sigma_+^2 + \sigma_+ N_+ \left( \frac{\partial \phi_+}{\partial z} - \frac{pw'}{\sigma_+^2} \left( m_+ \frac{\partial \sigma_+}{\partial z} - \sigma_+ \frac{\partial m_+}{\partial z} \right) + \frac{pw'^2}{\sigma_+^2} \frac{\partial \sigma_+}{\partial z} \right) - \frac{1}{2} \frac{\partial m_+}{\partial z} \left( 1 + \operatorname{erf} \left( \frac{w - m_+}{\sqrt{2}\sigma_+} \right) \right)$$

with the expressions for  $\phi_-$  of the same form, except with  $p$  replaced by  $1-p$  and with subscript "+" replaced by "-". Note that due to the relation between  $m_+$  and  $m_-$  the inner bracket in the second term is zero, and  $(1 + \operatorname{erf})$  can be replaced simply with  $\operatorname{erf}$ , when the + and - terms are combined.

### 5.3.3 Computational Timestep

It is necessary to define a computational timestep such that the change in magnitude of  $\sigma_w$  should be small in comparison to  $\sigma_w$  itself, i.e.

$$w' \Delta t \left| \frac{d\sigma_w}{dz} \right| \ll \sigma_w,$$

so that

$$\Delta t \ll \frac{1}{|d\sigma_w/dz|}.$$

For practical purposes

$$\Delta t = \frac{e_1}{|d\sigma_w/dz|},$$

where  $e_1$  is a small number such as 0.05 or 0.1. However, this may lead to large values near  $d\sigma_w/dz = 0$ , so it is replaced by

$$\Delta t = \frac{e_1 z_i}{|w'|}$$

if it is smaller, where  $z_i$  is the boundary layer depth (replaced by  $z$  if  $z > z_i$ ).

In addition, the timestep must be short in comparison with the Lagrangian timescale, so that the additional restraint of

$$\Delta t \leq e_2 \tau_w$$

is applied, where  $e_2$  is another small number. In order to avoid too short a timestep, the Lagrangian timescales for all stabilities are subject to a minimum of 20 seconds, although in reality they may well be smaller near the surface.



### 5.3.4 Long Range Scheme

The random walk technique is computationally expensive, so a simpler scheme is used at longer ranges. A fixed timestep  $\Delta t_d$  is used (i.e the timestep of the main loop--- Section 3.1, typically 5, 10 or 15 mins), and the turbulent component is determined under the assumption  $\Delta t = \tau$  so that the memory term is excluded (see expression 5.3). Values for  $\sigma$  and  $\tau$  (horizontal and vertical) are determined from homogeneous profiles, and an effective velocity variance  $\sigma_{eff}$  determined appropriate to the timestep  $\Delta t_d$ , which preserves an appropriate diffusion coefficient  $K$ . That is,

$$K = \sigma^2 \tau = \sigma^2 \Delta t = \sigma_{eff}^2 \Delta t_d$$

then

$$\sigma_{eff} = \sqrt{\frac{\sigma^2 \tau}{\Delta t_d}},$$

and from equation 5.3 ,

$$u' = \sqrt{2} \sigma_{eff} r_t.$$

Similarly for the other components. Advection is then by equation 5.1, producing, of course, the parabolic spread which results from this type of formulation.

## 5.4 Turbulence profiles

The remainder of the formulation consists of the derivation of suitable values for the vertical profiles of  $\sigma$  and the Lagrangian timescale  $\tau$  or turbulence dissipation rate  $\varepsilon$ . These will depend on the stability of the atmospheric boundary. As turbulent kinetic energy is not available from the Unified Model, the values must be determined either from empirical fits to observational data, or parametrized from information available from the Unified Model, e.g. by Richardson number formulae. The first option has been chosen for the NAME II parametrization. For the unstable boundary layer, we employ the turbulence profiles of Hibberd and Sawford (1994) and Hurley and Physick (1993), with a mechanical component or neutral limit from Brost et al (1982).

Both inhomogeneous profiles (i.e.  $\sigma$  &  $\tau$  a function of height within the boundary layer) and homogeneous profiles (i.e.  $\sigma$  &  $\tau$  constant within the boundary layer) are available. The inhomogeneous profiles are the most accurate whilst the use of homogeneous profiles offers the advantage of computational speed.

### 5.4.1 Determination of Stability

The stability of the boundary layer is determined from the Monin-Obhukov length:

$$L = -\frac{c_p T_s u_*^3}{kgH}$$



where  $c_p$  is the specific heat at constant pressure,  $k$  is von Karman's constant,  $T_s$  the surface temperature,  $H$  the sensible heat flux and  $u_*$  the friction velocity. Negative values of  $L$  indicate unstable boundary layers.

## 5.4.2 Stable Conditions

### 5.4.2.1 Inhomogeneous profiles

At night the atmosphere becomes stably stratified due to radiative cooling from the surface beneath, and turbulence tends to be suppressed. Typically it takes the form of slow oscillations of wind direction with intermittent bursts of mechanically driven turbulence, depending on the wind strength. The profiles adopted for the present are (Hanna 1982)

$$\sigma_u = \sigma_v = 2.0u_* \left(1 - \frac{z}{z_i}\right)$$

$$\sigma_w = 1.3u_* \left(1 - \frac{z}{z_i}\right)$$

$$\frac{d\sigma_w}{dz} = -\frac{1.3u_*}{z_i};$$

and the Lagrangian timescales

$$\tau_x = \tau_y = 0.07 \frac{z_i}{\sigma_v} \left(\frac{z}{z_i}\right)^{\frac{1}{2}}$$

$$\tau_w = 0.1 \frac{z_i}{\sigma_w} \left(\frac{z}{z_i}\right)^{0.8}$$

### 5.4.2.2 Homogeneous profiles

For the case of homogeneous turbulence (i.e. constant within the boundary layer), the following values are used:

$$\sigma_u = \sigma_v = u_*$$

$$\sigma_w = 0.65u_*$$

$$\tau_u = \tau_v = \tau_w = 0.05 \frac{z_i}{\sigma_u}$$

## 5.4.3 Unstable Conditions

Unstable or convective conditions occur where the air is buoyant due to heating from the surface. The boundary layer is deepened steadily by the action of thermals on the



capping inversion, and reaches a maximum (which may be a km or two) by late afternoon. Turbulent mixing is due to both buoyant overturning and mechanical turbulence, which decay in the mixed layer after sunset. When the weather conditions are generally overcast and windy, and in some situations of transition, the heat flux to and from the surface is near zero, and the atmosphere is described as neutral.

#### 5.4.3.1 Inhomogeneous turbulence

For skewed inhomogeneous turbulence the vertical velocity variance is determined from Hibberd and Sawford's (1994) profile adjusted to include a component for the mechanical generation of turbulence (by way of a sum of squares) using a mechanical term derived from the profiles in Brost et al (1982):

$$\sigma_w = \left[ 12w_*^2 \left( 1 - 0.9 \frac{z}{z_i} \right) \left( \frac{z}{z_i} \right)^{\frac{2}{3}} + \left( 1.8 - 1.4 \frac{z}{z_i} \right) u_*^2 \right]^{\frac{1}{2}}$$

so that

$$\frac{d\sigma_w}{dz} = \frac{1}{\sigma_w z_i} \left\{ w_*^2 \left( \frac{z}{z_i} \right)^{-\frac{1}{3}} \left( 0.4 - 0.9 \frac{z}{z_i} \right) - 0.7 u_*^2 \right\}$$

These formulae can also, of course, be applied in the neutral limit. A.R. Brown (private communication) has found from LES integrations that although formulae which exclude the mechanical contribution are inadequate, the inclusion of the full neutral component can give results which are a little excessive. A cube root sum of cubes may be preferable. The formulae will be reviewed when further experience has been gained. Similarly,

$$\sigma_u = \sigma_v = \left[ 0.4w_*^2 + (5 - 4z/z_i)u_*^2 \right]^{\frac{1}{2}}$$

It will be noted these formulae give a profile for  $\sigma$  up to about  $z/z_i = 1.3$ . In addition,  $Sk=0.6$  and  $C_\sigma=1.0$ ---this value was found to give better results than  $C_\sigma = 2$  for the NAME II model.

The formula for the dissipation rate of TKE is a combination of convective and neutral terms from Luhar and Britter (1989) and a fit to the profile in Grant (1992), respectively:

$$\varepsilon = \left( 1.5 - 1.2 \left( \frac{z}{z_i} \right)^{\frac{1}{3}} \right) \frac{w_*^3}{z_i} + \frac{u_*^3 (1 - 0.8z/z_i)}{kz}$$

subject to a minimum of  $10^{-6}$ , and



$$\tau_{u,v,w} = 2\sigma_{u,v,w}^2 / C_0 \varepsilon$$

#### 5.4.3.2 Homogeneous turbulence

For the simpler case of Gaussian homogeneous turbulence the profiles used are

$$\sigma_u = \sigma_v = [0.4w_*^2 + 3u_*^2]^{1/2}$$

$$\sigma_w = [0.4w_*^2 + 1.1u_*^2]^{1/2}$$

$$\varepsilon = 0.6w_*^3 / z_i + 1.2u_*^3 / kz_i$$

used to compute  $\tau$ , as above;  $Sk=0.0$ , and  $C_0 = 1.0$ .

#### 5.4.4 Free troposphere

Above the boundary layer fixed values are currently used:

$$\sigma_u = 0.5 \text{ms}^{-1}$$

$$\tau_u = 600 \text{s}$$

$$\sigma_w = 0.1 \text{ms}^{-1}$$

$$\tau_w = 300 \text{s}$$

This is an area of ongoing investigation.

### 5.5 Boundary Conditions

For each call to the advection routines particles are advected through a model timestep (typically 5, 10 or 15 minutes), either by a series of shorter variable timesteps (near-source scheme) or by a single step (long-range scheme).

When using homogeneous profiles particles are maintained within the boundary layer during a model timestep by reflecting particles off the surface and boundary layer top. In unstable conditions where the skewed turbulence is applied then the boundary condition used is one of skewed memory reflection, where  $w'$  is scaled by the absolute value of the ratio of the mean updraft velocity to the mean downdraft velocity when reflecting at the ground ( $w'$  becomes  $-w'(1-p)/p$ ). The inverse of this ratio is used in an analogous manner at the top of the mixed layer. Mixing across the boundary layer top therefore occurs through the movement of the boundary layer top from one model timestep to the next, or by particles in the boundary layer being advected to regions of differing boundary layer depths. In either case the turbulent components are reinitialised.

When using inhomogeneous profiles particles are reflected from the surface as in the homogeneous case, but are not reflected at the boundary layer top, or reinitialised on



passage through the inversion, as  $\partial\sigma_w / \partial z$  is (at least piecewise) continuous.

Turbulent components *are* reinitialised if particles cross the boundary layer top due to the boundary layer depth changing between timesteps ( $\partial\sigma_w / \partial t$  is discontinuous)--- in both homogeneous or inhomogeneous situations. The topic of entrainment is scheduled for further investigation.

## 5.6 Plume Rise.

A method of incorporating plume rise and inversion penetration has been developed based upon the work of G.A.Briggs (see Randerson 1984, Seinfeld 1986 and J.C.Weil in Venkatram and Wyngaard (eds) 1988). This was done in collaboration with F.B.Smith (Imperial College), and was designed to utilise the multiple particle structure of the model and the diffusion code.

### 5.6.1 Unstable or neutral conditions.

The strategy adopted is to recognise that the wind at the stack top is not constant; when the fluctuating velocity is weak the plume temperature will be higher and the plume rise (for a short period) greater. The individual particles will have a random scatter about the middle of this fluctuating plume height. The fluctuating plume rise  $h(t)$  is from

$$h(t) = \left\{ \frac{3r_0^2 T_a R^2 X}{(0.4 + 1.2/R)^2 T_s} + \frac{3}{2} \frac{g(T_s - T_a) v_s r_0^2 X^2}{0.36 T_a U^3} \right\}^{1/3}, \quad (5.12)$$

where  $r_0$  is the stack radius,  $v_s$  the emission velocity, the current wind strength

$$U = \left\{ (\bar{u} + u')^2 + (\bar{v} + v')^2 \right\}^{1/2},$$

$X$  is the distance from source computed using  $U\Delta t$ ,  $R = v_s / U$ ,  $g$  is the gravitational acceleration and  $T_a, T_s$  the ambient air and emission temperatures respectively. Then the plume height is  $z_{pl}(t) = h(t) + h_s$ , where  $h_s$  is the height of the stack. The two terms on the RHS represent momentum and (of much greater importance here) plume buoyancy. To compute the displacement of particles scattered about the centreline of the instantaneous plume, it is assumed

$$h_p(t + \Delta t) = h_p(t) + [h(t + \Delta t) - h(t)] + h'(t)$$

where  $h_p$  is the particle rise and the random increment,  $h'$ , is generated from a Gaussian distribution with zero mean and standard deviation

$$\sigma_p = 0.14 [h(t + \Delta t)^2 - h(t)^2]^{1/2},$$



i.e.,  $h' = r\sigma_p$ , where  $r$  is a random variable mean zero, standard deviation 1.  $\sigma_p$  is derived under the assumption that the plume width  $W(t) \approx 0.6h(t)$ . Then the new particle height  $z_p$  is from

$$z_p(t + \Delta t) = z_p(t) + h(t + \Delta t) - h(t) + h'(t) + w(t),$$

where  $w = \bar{w} + w'$  is the vertical component which includes the ambient mechanical turbulence, and allowance is made for reflection from the surface. The application of both the turbulent velocity components and fluctuations due to buoyancy ( $h'$ ) to the particle displacements may seem excessive, as they are not additive in any simple way; however, preliminary tests suggested that a realistic spread is obtained, with  $w$  offering only a small (but coherent) addition to  $h'$  (which tends to increase with distance from the source). Nonetheless the inclusion of  $w$  noticeably increases the vertical spread  $\sigma_z$  (by around 15% in the tests carried out).

The mass flux from the chimney is from  $F_m = \pi r_0^2 v_s$ , and the plume temperature after a period  $t$  is estimated as

$$T_p(t) = \{F_m T_s + (F_m(t) - F_m) T_a\} / F_m(t),$$

where  $F_m(t) = \pi W(t)^2 U / 4$ .

Once  $z_p$  is obtained the plume temperature  $T_p(t)$  is tested against the temperature just above the inversion,  $T_{zi}$ , and the particle height tested against the inversion height  $z_i$ . Then

- (i) if  $T_p(t) < T_{zi}$  then the plume rise is terminated, the particle assumed passive, and the usual advection continued;
- (ii) if  $z(t) > z_i$  then the particle is transferred to the level at which it is neutrally buoyant, and continued as a passive particle;
- (iii) if both tests fail the plume rise is continued.

### 5.6.2 Stable conditions.

In stable conditions expression 5.12 is replaced with  $h(t) = \varepsilon X^\beta / U^\alpha$  where the parameters are from

$\alpha$	$\beta$	$\varepsilon$
1/3	0	$2.4(F/S)^{1/3}$
0	0	$5F^{1/4}S^{-3/8}$
1	2/3	$1.6F^{1/3}$



where  $F$  the buoyancy flux parameter is  $g\tau_0^2 v_s [T_s - T_a] / T_s$ ,  $S$  the stability parameter is from  $g \frac{d\theta}{dz} / T_a$ , and  $\theta$  is potential temperature.

## 5.7 Implementation

The full random walk technique is applied to near-source particles, where an accurate description of plume growth is most important. At present the technique is applied to particles for a user-defined time period following release, chosen (e.g.) to represent the time required for particles to become well mixed through the boundary layer. For a given particle inhomogeneous profiles are used for an initial period  $t_{in}$ , then homogeneous profiles are used for a subsequent period of  $t_h$ . Finally, after a period of  $t_{in} + t_h$ , the long range scheme is applied, using homogeneous profiles. Note that any combination of profiles can be used by setting either or both of  $t_{in}$  and  $t_h$  to zero.

The skewed turbulence option in unstable conditions can be applied whether homogeneous or inhomogeneous profiles are used, for a user defined period of  $t_{sk}$  (subject to  $t_{sk} \leq t_{in} + t_h$ ). In this way an optimum timestep can be used at the various stages of a simulation while still reproducing the essential features of dispersion.

## 5.8 Poles

For the global grid problems are possible near the polar regions. This arises because cell lengths in the east-west direction are very small. The  $u$  velocity component can cause a particle to 'spin' around the pole many times if it is very close to the pole. To prevent this the  $u$  component of both the velocity and the random perturbation due to diffusion is set to zero for particles close to the poles. The  $v$  velocity component is interpolated from the nearest two grid values.

With a latitude/longitude grid, as for the global version, the horizontal random walks can result in some slight poleward bias (D.J. Thomson, personal communication, has examined this situation). This could be a matter for concern in prolonged integrations, but it is considered that the NAME model is not significantly affected for periods of a day or more as the spread of particles is primarily by the resolved winds, diffusion playing a relatively minor role (Maryon & Buckland, 1995).

## 5.9 Mixing by Convection

One potentially important mechanism for mixing particles in the vertical is convection. Material can be rapidly transported upwards throughout the depth of the atmosphere during deep convection, removing material from the boundary layer. Similarly, material can be brought down from upper layers by compensating downdraughts (generally weaker, but over larger areas). Whilst a detailed understanding of the role of deep convection in redistributing pollutant in the vertical is not available, a simple scheme has been introduced to represent this enhanced vertical mixing.

If convective cloud is present, a particle between the cloud base and the convective cloud top level is given a probability proportional to the convective cloud amount of



being given an additional vertical velocity component. The vertical velocity component is taken from a Gaussian distribution of mean zero, with variance  $1\text{ms}^{-1}$  at the cloud base, linearly decreasing to a variance of  $0\text{ms}^{-1}$  at the cloud top. Work is currently underway to improve this scheme.

## 6. LOSS PROCESSES

### 6.1 Introduction

The processes by which material is lost from the atmosphere in the NAME model include wet and dry deposition to the ground, radioactive decay and chemical reactions. Within the model these losses are applied on a particle basis, i.e. the mass of each particle is reduced each timestep, and for deposition processes the depleted mass added to surface deposition maps.

### 6.2 Wet Deposition

For many pollutants wet deposition is the dominant means by which material is removed from the atmosphere to the ground. Two main processes are involved: washout, where material is 'swept out' by falling precipitation; and rainout (the most efficient), where material is absorbed directly into cloud droplets as they form by acting as cloud condensation nuclei. Rainout coefficients are dependent on the phase (i.e. water or ice/snow) and on the mechanisms for droplet growth, which differ for dynamic and convection clouds. Washout coefficients are also dependent on the precipitation type, for example snow flakes 'sweep' out a larger area than rain drops. Enhanced removal occurs where precipitation is orographically enhanced by the seeder/feeder mechanism.

The removal of material from the atmosphere by wet deposition processes is based on the depletion equation

$$\frac{dC}{dt} = -\Lambda C$$

where  $C$  is the air concentration,  $t$  is time, and  $\Lambda$  is the scavenging coefficient. The mass by which each particle is depleted can then be given by

$$\Delta m = m(1 - \exp(-\Lambda \Delta t)) \quad (6.1)$$

where  $m$  is the mass of the particle at the start of the timestep. The scavenging coefficient  $\Lambda$  is usually defined by:

$$\Lambda = Ar^B \quad (6.2)$$

where  $r$  is the rainfall rate and  $A$  and  $B$  are coefficients defined for different types of precipitation (e.g. dynamic, convective, rain and snow), and different deposition processes (e.g. rainout, washout and orographically enhanced precipitation).



## 6.2.1 Scavenging Coefficients

Table 7.1 summarises the scavenging coefficients currently implemented within the model and when they are applied. The coefficients, based on observational data and detailed cloud modelling, have been supplied by Dr T Choularton at UMIST, who has collaborated with the NAME team over a long period.

Note that orographically enhanced rainfall coefficients are used only where (i) the precipitation data originate from FRONTIERS processed data (i.e. only over the UK); (ii) orographic enhancement has been applied to the FRONTIERS data; and (iii) the relief is greater than 150 m.

	$\Lambda(\text{s}^{-1})$ Rain (Below Freezing Level)		$\Lambda(\text{s}^{-1})$ Snow (Above Freezing Level)		When Applied
	Convective	Dynamic	Convective	Dynamic	
Washout	$8.4 \times 10^{-5} r^{0.79}$		$8.0 \times 10^{-5} r^{0.305}$		-Below Cloud base
Rainout	$3.36 \times 10^{-4} r^{0.79}$	$8.4 \times 10^{-5} r^{0.79}$	$3.36 \times 10^{-4} r^{0.79}$	$8.0 \times 10^{-5} r^{0.305}$	-Between cloud base and cloud top
(Seeder/ Feeder)	$3.36 \times 10^{-4} r^{0.79} +$		$1.0 \times 10^{-3} r^{0.79}$		-Below 1200 m, -Topography > 150m -FRONTIERS Orographic flag

Table 6.1 Scavenging coefficients used in the name model,  $r$  is rainfall rate (mm/hr)

## 6.2.2 Meteorological data

### Precipitation

All relevant met data (e.g. precipitation rates, cloud details) are linearly interpolated in space to particle positions, and in time to the start of the current model time step. When requested and available hindcast precipitation rates are taken from the nearest high resolution precipitation value, interpolated in time. As the high resolution precipitation fields do not distinguish between convective and dynamic precipitation, the model ratio of convective to dynamic precipitation is used to apportion the precipitation.

Both instantaneous precipitation rates at data times and accumulations between data times are available from the Unified Model. Whilst rates give an accurate description of the precipitation at data times, they provide no information about the precipitation between those times. In contrast, accumulations give an accurate representation of the total precipitation between data times but no information as to its distribution in time. A simple scheme is therefore used to combine these two sources of precipitation data. If  $r_1$  and  $r_2$  are the instantaneous rates at adjacent data times  $\Delta t$  apart, and  $A$  is the model accumulation over  $\Delta t$ , then the rates used  $r_{1,eff}$  and  $r_{2,eff}$  are determined from



$$\frac{r_{1,eff}}{r_1} = \frac{r_{2,eff}}{r_2} = \frac{A}{0.5(r_1 + r_2)\Delta t}$$

i.e. the rates  $r_1$  and  $r_2$  are scaled so that the accumulation over  $\Delta t$  derived from the rates equals the accumulation  $A$ . The convective and dynamic rates are scaled separately. Options exist to use either rates or accumulations only.

### Cloud

Convective cloud amount, cloud base and top are interpolated from adjacent model grid point values. As dynamic cloud information is unavailable from the Unified Model, fixed pressure levels of 900 hPa and 700 hPa are currently used for the dynamic cloud base and top.

The temperature at the particle position is used to determine whether the particle is above or below the freezing level ( $0^\circ\text{C}$ ).

### 6.2.3 Implementation

Appropriate values for the coefficients  $A$  and  $B$  (equation 6.2) are determined separately for convective and dynamic precipitation, depending on the particle height relative to the appropriate cloud base, cloud top and freezing level. The coefficients for snow/ice are used above the freezing level, and coefficients for rain below the freezing level. The convective precipitation rate will generally underestimate the true convective precipitation rate, as it represents the mean rate over the whole grid cell, even though the precipitation may only be occurring over a fraction of the area. The convective precipitation rates  $r_{con}$  are therefore obtained from

$$r_{con} = r / f_c,$$

where  $f_c$  is the convective cloud amount fraction. The particle mass is then depleted for each species according to Equation (6.1) for both the convective and dynamic precipitation components. For convective precipitation the depletion is applied to the fraction  $f_c$  of the particle mass.

The total depleted mass for each species is integrated for each of the wet deposition fields, and expressed as a deposition per unit area.

### 6.3 Dry Deposition

Whilst wet deposition is the dominant loss process for most pollutants, dry deposition is still an important loss process. The basis of the parametrization is that the flux  $F$  of pollutant to the ground is proportional to the concentration  $C$  of the pollutant above the ground:

$$F = v_d C$$



where the constant of proportionality  $v_d$  is known as the deposition velocity. Both  $v_d$  and  $C$  are defined at a reference height  $z$ , typically 1-2m. Assuming that concentrations are constant over a surface layer of depth  $z_s$ , then

$$\frac{dC}{dt} \approx -\frac{F}{z_s} = -\frac{v_d}{z_s} C$$

where  $t$  is time. The mass loss for a particle within the layer  $z_s$  can then be written as

$$\Delta m = \frac{v_d}{z_s} m \Delta t.$$

Currently  $z_s$  is taken as the boundary layer depth.

### 6.3.1 Deposition Velocity $v_d$

A resistance analogy parametrization is used to determine the deposition velocity at each particle position:

$$v_d = \frac{1}{R_a + R_b + R_c}$$

where  $R_a$  is the aerodynamic resistance,  $R_b$  is the laminar layer resistance, and  $R_c$  is the surface resistance.

#### Aerodynamic Resistance

The aerodynamic resistance is used to specify the efficiency with which material is transported to the ground by turbulence, and is independent of the pollutant type. A commonly used expression is

$$R_a = \frac{1}{ku_*} \left[ \ln \left( \frac{z+z_0}{z_0} \right) - \Psi_h \left( \frac{z+z_0}{L} \right) \right]$$

where  $k$  is von Karmans constant (0.4),  $u_*$  is surface stress,  $z_0$  is the roughness length and  $L$  is the Monin-Obukhov length.  $\Psi_h$  is a stability correction function for temperature, defined here in unstable conditions by

$$\Psi_h = 2 \ln \left[ \frac{(1 + \phi_m^2)}{2} \right]$$

where

$$\phi_m = \left( 1 - 16 \frac{z+z_0}{L} \right)^{1/4};$$

in stable conditions by



$$\Psi_h = -5 \left( \frac{z + z_0}{L} \right).$$

In the limits as  $|L|$  becomes large  $\Psi_h$  tends to zero, and the conditions approximate neutral.

### Laminar Resistance

The laminar resistance represents the resistance to transport across the thin quasi-laminar layer adjacent to the surface. For gaseous pollutants, and the range of particulates  $0.1 - 10 \mu\text{m}$  (of particular relevance to releases of a number of radioactive species such as caesium), we take

$$R_b = \frac{2}{0.72ku_*} \left( \frac{\nu}{D_i} \right)^{2/3}$$

where  $\nu$  is the kinematic viscosity of air ( $0.15 \text{cm}^2 \text{s}^{-1}$ ) and  $D_i$  is the molecular diffusivity of pollutant. For practical purposes it is reasonable to approximate  $R_b$  to a fixed value: i.e.

$$R_b = \frac{8}{u_*}.$$

### Surface Resistance

The surface resistance characterises the resistance to capture by the surface itself. It is often the most important of the resistances, yet it represents a complex process and remains the least well understood. It depends both on the pollutant and on the nature of the surface (e.g. crops, forest, concrete etc.), which may itself be dependant on other factors (e.g. season, time of day, atmospheric conditions etc., see Erisman 1994, Baldocchi et al 1987 & Baer & Nester 1992).

Given the uncertainties in determining surface resistance and the wide range of values found in the literature (e.g. Walcek et al 1986, Sehmel 1980), a fixed value of  $R_c$  is used for each species, as listed in Table 5. In general, the more reactive a species the lower its surface resistance.

### 6.3.2 Gas to particulate conversion.

After emission, iodine-131 gas is steadily taken up by particulate aerosol, with a corresponding alteration to the deposition velocity. Starting with equations for the time rate of change of gaseous and particulate concentration it is possible to derive an expression for the net loss of  $I_{131}$ :

$$\frac{dC}{dt} = - \left( \frac{v_d}{z_s} + \frac{1}{\tau} \right) C(t) + \frac{C_g(0)}{\tau} \exp \left( - \frac{w_d}{z_s} t \right)$$



where  $C_g(0)$  is the initial concentration of the gas and  $v_d$ ,  $w_d$  are the gaseous and particulate deposition velocities, respectively. The conversion timescale  $\tau$  has been estimated at 47 days for the emissions from Chernobyl reaching Britain.

#### 6.4 Turbulent Deposition

Turbulent (or occult) deposition occurs where 'polluted' cloud droplets directly impact to the ground. This generally occurs when moist low level air is saturated to form hill capping cloud as it is advected and lifted over higher ground. Whilst strictly a wet deposition process occult deposition is parametrized in terms of a dry deposition velocity. The dry deposition velocity used is related to the value for momentum (as determined in field observations by T. Choularton's team at UMIST) i.e.:

$$v_d = \frac{0.8}{R_a}$$

Turbulent deposition is only applied where the liquid water content is greater than  $10^{-4}$  kg/kg, the friction velocity  $u_*$  is greater than 0.2 m/s (to avoid applying occult deposition in regions with radiation fog), and where the relief exceeds 150 m.

#### 6.5 Radioactive Decay

For radioactive materials mass is lost by radioactive decay. The governing equation is

$$\frac{dm}{dt} = -\frac{m}{aq}$$

where  $q$  is the half-life,  $a$  is a constant ( $=1.4427$ ). The mass of a particle can then be written as

$$m_2 = m_1 \left( 1 - \frac{\Delta t}{aq} \right)$$

### 7. AUTOMATIC ADJUSTMENTS TO MODEL PRODUCTS

As a consequence of model error, forecast error and the natural randomness and variability of the atmosphere the model meteorology will always differ from reality to some extent. NAME II has several facilities for modifying the model products---and assumptions of source strength---by comparing the model output with the observations of radioactivity which would be made widely in the event of a serious nuclear accident. One facility (manual rather than automatic) is to 'bend' the near-source plume by biasing the random walk, if the real plume is observed to set off at an angle to the simulated one. There are also automated facilities for adjusting the plume spread by means of an artificial 'diffusivity' and for estimating the strength of a source from measured concentration data. Given reasonably complete observed and model predicted air concentration fields at a given time, a least squares technique can be used to estimate the source strength, both as a function of time and height. Thus there



are two main stages: (i) plume spread adjustments and (ii) source reconstitution; these are discussed in sections 7.1 and 7.2. A full description of the technique can be found in Maryon and Best (1995).

## 7.1 Plume spread

The model inaccuracies are likely to be particularly serious where the winds are strong, and rapidly changing, as near an active, travelling depression. The area over which the model predicted plume overlaps with the observed field is likely to be insufficient in these circumstances. To improve the overlap the model is re-run iteratively, adjusting the diffusion coefficient (up or down) to obtain an overlap between the observed and model air concentration fields between 95 and 100%. The downward adjustment may be required to prevent unrealistically wide spreads of model particles before a near 100% coverage is obtained. The change in diffusion coefficient is related to the time rate of change of wind velocity, as errors are likely to be related to the magnitude of the wind shift: i.e. a modified diffusion coefficient  $K'$  used for each particle is calculated from

$$K' = (\beta|\varepsilon| + K^{\frac{1}{2}})^2$$

where  $\beta$  is an arbitrary user-defined coefficient,  $\varepsilon$  is the wind change at the particle location, and  $K$  is the diffusion coefficient. As  $K$  is defined in terms of the velocity variance  $\sigma$  and Lagrangian timescale  $\tau$  this becomes

$$\sigma'^2 \tau = (\beta|\varepsilon| + \sqrt{\sigma^2 \tau})^2$$

where  $\sigma'^2$  is a modified velocity variance. The value of  $\beta$  is changed using an iterative scheme until a suitable overlap is found.

## 7.2 Source reconstitution

The source emission profile is broken down into  $M$  'slots', each describing a time window and vertical slab for which an estimated emission is required. Two vertical slabs are probably the most that can be realistically adopted. Let the model emissions for each slot be  $e_i'(0)$ ,  $i=1,2..M$  and the corresponding 'real' emissions  $e_i(0)$ ,  $i=1,2..M$ ; then at a given time  $t$  in a particular grid cell,  $j$ ,

$$\sum_{i=1}^M a_{ij} e_i(0) = A_j$$

where  $A_j$  is the measured activity/mass in the grid-cell  $j$ , and  $a_{ij}$  are coefficients representing the proportion of each  $e_i(0)$  contributing to  $A_j$ . Then if there are  $N$  grid cells with observed mass, and  $N > M$ , a least squares solution for  $e_i(0)$  can be found (Maryon and Best (1995). Introducing a weighting,  $\omega_j$ , to represent the confidence in the model simulation for grid cell  $j$ , we minimise



$$\sum_{j=1}^N \omega_j \left[ A_j - \sum_{i=1}^M \alpha_{ij} e_i(0) \right]^2$$

yielding the 'normal equations'

$$\frac{d}{d[e_p(0)]} \left[ \sum_{j=1}^N \omega_j \left( A_j - \sum_{i=1}^M \alpha_{ij} e_i(0) \right)^2 \right] = 0 \quad p = 1, 2, \dots, M.$$

From this the linear system

$$\sum_{i=1}^M e_i(0) \sum_{j=1}^N \omega_j \alpha_{pj} \alpha_{ij} = \sum_{j=1}^N \omega_j \alpha_{pj} A_j \quad (7.1)$$

is derived, which can be solved for the  $e_i(0)$  using matrix operations.

The weighting factors  $\omega_j$  are currently based on the average ratio of final to initial particle mass for all particles within the grid cell; thus grid cells in which particles have lost a significant fraction of their mass due to depletion processes (and are therefore less reliable) contribute less to the solution. Later the reliability of observations may be incorporated in the weighting. Processing of radiological data to produce fields conformable with the structure of NAMEII is by a software package supplied by AEA Technology Consulting Services, though at the time of writing this is yet to be brought into full operational use.

### 7.3 Implementation

Given that an observed air concentration field is available at time  $t_1$  resulting from a release at time  $t_0$ , a standard model simulation is performed from time  $t_0$  to  $t_1$  with release slots defined to correspond with each of the slots required for the emission reconstitution. A best guess of the emission rate, or default value, is used for each slot. At the end of the run the emission from each slot is calculated from equation 7.1, together with the overlap between the observed and model predicted air concentration fields. If the overlap is too small the value of  $\beta$  is incremented iteratively by a user-defined amount until it exceeds 95%. If it attains 99%  $\beta$  is decreased using a smaller decrement. Thus a coverage between 95 and 99% is obtained (anything larger is bound to be associated with excessive spread of the modelled plume). The number of iterations is confined to a user-defined maximum. At present this procedure can only be carried out for one time,  $t_1$ , during a model integration, so that repeated runs would be necessary to deal with subsequent observational fields.

## 8. OUTPUT

### 8.1 Fields

Fields of diagnosed data, such as air concentrations and depositions, can be calculated and output on any of the unified model grids, irrespective of the resolution of the



input data used to advect and deplete particles. In addition, fields can be output on (i) a 20 km resolution grid covering the UK based on the national grid (Figure 5); (ii) a user-defined latitude/longitude grid; and (iii) the high resolution rainfall grid. As well as diagnosed fields (Table 4 lists all available diagnosed fields) any meteorological field used in the model can be output. Fields are output at user-defined intervals (the minimum interval is the model timestep), based on either UTC times or on time since the start of release.

## 8.2 Time series

Detailed time series of diagnosed data and associated meteorological data can be generated at an arbitrary number of user-defined locations, with values generated each model timestep (met data are linearly interpolated from adjacent data times).

## 8.3 Profiles

In addition to fields and timeseries it is possible to generate vertical profiles of air concentrations or meteorological data. These are output at the same time intervals as the fields, for each of the locations time series data are requested.

## 8.4 Graphics

For APR purposes data are copied to a VAX or UNIX workstation for graphical display. A windows type interface has been written using the PV-WAVE data visualisation package to readily select and display model output.

Some example outputs from a nested model run are shown in Figures 7 to 10. The release is from 51 27N 002 35W starting at 1200UTC 22/07/1995 continuing for 96 hours, using mesoscale, regional and global NWP met data. The simulation was performed at 1800UTC 24/07/95, resulting in analysis (hindcast) data being used for the period 1200UTC 22/07/95 up until 1200UTC 24/07/95, after which forecast data was used. Mesoscale forecast data was available for the period 1200UTC 24/07/95 up to 1200UTC 25/07/95, regional forecast data from 1200UTC 24/07/95 up to 0000UTC 26/07/95 and global forecast data up to the end of the simulation. Thus over the UK the met data sources were: (i) mesoscale hindcast data for the period 1200UTC 22/07/95 to 1200UTC 24/07/95; (ii) mesoscale forecast data from 1200UTC 24/07/95 to 1200UTC 25/07/95; (iii) regional forecast data from 1200UTC 25/07/95 to 0000UTC 26/07/95; and finally (iv) global forecast data from 0000UTC 26/07/95 to 1200UTC 26/07/95. Figure 7 shows the final particle positions at 24 hour intervals; Figure 8 shows the averaged air concentrations, total dosage and accumulated wet and dry depositions at T+96 analysed on the regional grid. Figure 9 shows the total deposition field at T+96 analysed on the global, regional, mesoscale and national grids. Figure 10 shows time-series traces for air concentration, wet and dry deposition at Birmingham.

An example of a high resolution deposition field is shown in Figure 13. The release is from 51 24N 000 39W starting 0600UTC 26/07/95, continuing for 12 hours.



## 9. PLANNED MODEL IMPROVEMENTS

There are many areas in which the model could be improved and developed; this section briefly discusses the main topics that it is hoped will be addressed in the near future.

### 9.1 Platform

It is intended that the model will be implemented on the Met Office's CRAY computer during 1995. In addition to increased computational speed, increased memory will enable greater numbers of particles and species to be used - necessary for air pollution forecasting.

### 9.2 Meteorological data

(i) At present meteorological data are used from only a subset of the available NWP vertical levels. As increased computing memory and speed becomes available further vertical levels will be added for increased vertical resolution, especially on the regional and global grids.

(ii) During 1995/96 it is anticipated that improved high resolution precipitation images covering a wider area than at present will be available from the European radar network.

### 9.3 Advection and dispersion

(i) The diffusion scheme above the boundary layer (i.e. the free troposphere) is relatively simple, using fixed turbulent properties. This needs to be improved to identify the effects of strong wind shear, turbulence due to breaking gravity waves etc.

(ii) The optimum method for handling entrainments of material between the boundary layer and free troposphere will be investigated, including how to best treat the boundary layer top in the near-source diffusion schemes.

(iii) Improved parametrisation of vertical mixing by deep convection is required, with better estimates of vertical velocities as a function of height and cloud details.

### 9.4 Deposition

(i) The unified model calculates precipitation rates on a layer by layer basis, so the possibility of applying wet deposition on a layer by layer basis will be investigated. This might result in an improved representation of wet scavenging as a function of height, and would represent the effects of pollutant redistribution by the evaporation of precipitation. If this proves impractical, ways of generating better estimates of cloud base and top levels will be investigated for improved application of wet deposition (especially for dynamic precipitation).



- (ii) Further work on the surface resistance parametrisation is required for more accurate dry depositions.

## 9.1 Platform

It is intended that the model will be implemented on the Met Office's CRAY computer during 1992. In addition to increased computational speed, increased memory will enable greater numbers of particles and species to be used - necessary for air pollution forecasting.

## 9.2 Meteorological data

(i) At present meteorological data are used from only a subset of the available NWP vertical levels. As increased computing memory and speed becomes available further vertical levels will be added for increased vertical resolution, especially on the regional and global grids.

(ii) During 1992/93 it is anticipated that improved high resolution precipitation maps covering a wider area than at present will be available from the European radar network.

## 9.3 Advection and dispersion

(i) The diffusion scheme above the boundary layer (i.e. the free troposphere) is relatively simple, using fixed turbulent properties. This needs to be improved to identify the effects of strong wind shear, turbulence due to breaking gravity waves etc.

(ii) The optimum method for handling entrainment of material between the boundary layer and free troposphere will be investigated, including how to best treat the boundary layer top in the near-source diffusion schemes.

(iii) Improved parametrisation of vertical mixing by deep convection is required, with better estimates of vertical velocities as a function of height and cloud details.

## 9.4 Deposition

(i) The unified model calculates precipitation rates on a layer by layer basis, so the possibility of applying wet deposition on a layer by layer basis will be investigated. This might result in an improved representation of wet scavenging as a function of height, and would represent the effects of pollution redistribution by the evaporation of precipitation. If this proves important, ways of generating better estimates of cloud base and top levels will be investigated for both over and under cloud deposition (especially for dynamic precipitation).



# UNIFIED MODEL FIELDS USED IN NAME

Field	Units
Temperature (All levels)	K
U Component Of Wind (All levels)	ms <sup>-1</sup>
V Component Of Wind (All levels)	ms <sup>-1</sup>
W Component Of Wind (All levels)	$\dot{\eta}$
Specific Humidity (All levels)	gg <sup>-1</sup>
U Component Of 10m Wind	ms <sup>-1</sup>
V Component Of 10m Wind	ms <sup>-1</sup>
Surface & Mean Sea Level Pressure	Pa
Surface Heat Flux	Wm <sup>2</sup>
U Component Of Surface Stress	Nm <sup>2</sup>
V Component Of Surface Stress	Nm <sup>2</sup>
1.5m Temperature	K
1.5m Relative Humidity	Fraction(0-1)
Dynamic Rain Rate	mmhr <sup>-1</sup>
Convective Rain Rate	mmhr <sup>-1</sup>
Dynamic Snow Rate	mmhr <sup>-1</sup>
Convective Snow Rate	mmhr <sup>-1</sup>
Dynamic Rain Hourly Accumulation	mm
Convective Rain Hourly Accumulation	mm
Dynamic Snow Hourly Accumulation	mm
Convective Snow Hourly Accumulation	mm
Roughness length	m
Convective Cloud Amount	Fraction (0-1)
Convective Cloud Base	Pa
Convective Cloud Top	Pa
High Resolution Precipitation Rate	mmhr <sup>-1</sup>
High resolution precipitation Source	Source code
High Resolution Orographic enhancement flag	On/Off

Table 1a List of Unified model data used in NAME model



### MESOSCALE GRID VERTICAL LEVELS

Full levels		
NWP Level	$\eta$	AP <sub>0</sub>
10m	0.99880	0
2	0.99525	0
3	0.98820	0
4	0.97769	0
5	0.96494	0
6	0.94899	0
7	0.93049	0
8	0.91099	0
9	0.89049	0
10	0.86898	0
11	0.84648	0
12	0.82248	43.960
13	0.79497	248.72
14	0.76245	728.21
15	0.72493	1556.56
16	0.68241	2785.04
17	0.63488	4427.27
18	0.58235	6442.59
19	0.52730	8620.51
20	0.47230	10701.93
21	0.41474	12576.38
22	0.35470	14006.97
23	0.29975	14688.05
27	0.09925	8861.73

Half levels		
NWP Level	$\eta$	AP <sub>0</sub>
2.5	0.99290	0
3.5	0.98350	0
4.5	0.97190	0
5.5	0.9580	0
6.5	0.9400	0
7.5	0.9210	0
8.5	0.9010	0
9.5	0.8800	0
10.5	0.8580	0
11.5	0.8350	0
12.5	0.8100	87.762
13.5	0.7800	408.965
14.5	0.7450	1045.71
15.5	0.7050	2064.07
16.5	0.6600	3500.36
17.5	0.6100	5345.52
18.5	0.5550	7527.39
19.5	0.5000	9700.14
20.5	0.4450	11689.93
21.5	0.3850	13447.68
22.5	0.3250	14555.11
24.5	0.2250	14342.00
27.5	0.0750	7176.03

### LIMITED AREA GRID VERTICAL LEVELS

Full levels		
NWP Level	$\eta$	AP <sub>0</sub>
10m	0.9988	0
1	0.9970	0
2	0.9750	0
3	0.9304	0
4	0.8698	0
5	0.7922	472.5
6	0.6996	2408.0
7	0.5995	5809.3
8	0.5045	9469.9
11	0.2998	14688.0
15	0.0992	8861.7

Half levels		
NWP Level	$\eta$	AP <sub>0</sub>
1.5	0.994	0
2.5	0.956	0
3.5	0.905	0
4.5	0.835	0
5.5	0.750	939.0
6.5	0.650	3852.2
7.5	0.550	7727.9
9.5	0.385	13447.6
11.5	0.275	14818.3
13.5	0.175	12997.5
16.5	0.04	4000.0

Table 2a & b Mesoscale and Limited area grid levels used in NAME II



# GLOBAL GRID VERTICAL LEVELS

Full levels			Half levels		
NWP Level	$\eta$	AP <sub>0</sub>	NWP Level	$\eta$	AP <sub>0</sub>
10m	0.9988	0	1.5	0.994	0
1	0.9970	0	2.5	0.956	0
2	0.9750	0	3.5	0.905	0
3	0.9304	0	4.5	0.835	0
4	0.8698	0	5.5	0.750	939.0
5	0.7922	472.5	6.5	0.650	3852.2
6	0.6996	2408.0	7.5	0.550	7727.9
7	0.5995	5809.3	9.5	0.385	13447.6
8	0.5045	9469.9	12.5	0.225	14342.7
11	0.2998	14688.0	15.5	0.075	7176.0
15	0.0992	8861.7			

Table 2c Global grid vertical levels used in NAME II

## DIAGNOSIS LEVELS

Level	$\eta$ Range
1	1.0000-0.9970
2	0.9970-0.9750
3	0.9750-0.9304
4	0.9304-0.8698
5	0.8698-0.7922
6	0.7922-0.6996
7	0.6996-0.5995
8	0.5995-0.5045
9	0.5045-0.2998
10	0.2998-0.0000

Table 3 Output diagnosis levels on all grids



## OUTPUT DIAGNOSTIC FIELDS

Diagnostic fields	
Air concentrations at all diagnostic levels	
Boundary layer air concentrations	
Free troposphere air concentrations	
Boundary layer dosages	
Dry deposition to the ground	
Wet deposition to the ground	
Total deposition to the ground	
High resolution wet deposition	

Table 4 Output diagnosis fields

SPECIES	Half Life/hrs	Rc/sm <sup>-1</sup>
Cobalt-58	1699.0	0
Cobalt-60	46170.0	0
Krypton-85	937000.0	∞
Krypton-85m	4.5	∞
Krypton-88	2.8	∞
Rubidium-86	446.0	0
Strontium-89	1212.0	0
Strontium-90	254900.0	0
Strontium-91	9.5	0
Yttrium-90	64.1	0
Yttrium-91	1406.0	0
Zirconium-95	1572.0	0
Niobium-95	842.4	0
Zirconium-97	16.9	0
Molybdenum-99	66.0	0
Technetium-99m	6.0	0
Ruthenium-103	945.6	1000
Ruthenium-105	4.4	1000
Rhodium-105	35.3	0
Ruthenium-106	8832.0	0
Antimony-127	93.4	0
Antimony-129	4.3	0
Tellurium-127	9.4	1000
Tellurium-127m	2616.0	1000
Tellurium-129	1.2	1000
Tellurium-129m	806.4	1000
Tellurium-131m	30.0	1000
Tellurium-132	78.2	1000

Table 5 Species half lives and R<sub>c</sub> values



SPECIES	Half Life/hrs	Rc/sm <sup>-1</sup>
Iodine-131	193.0	150
Iodine-132	2.3	50
Iodine-133	20.8	50
Iodine-134	0.9	50
Iodine-135	6.6	50
Xenon-133	126.0	∞
Xenon-135	9.1	∞
Caesium-134	18050.0	1000
Caesium-136	316.8	1000
Caesium-137	262800.0	1000
Barium-140	304.8	0
Lanthanum-140	40.3	0
Cerium-141	780.0	0
Cerium-143	33.0	0
Cerium-144	6840.0	0
Praseodymium-143	326.4	0
Neodymium-147	262.0	0
Neptunium-239	56.6	0
Plutonium-238	768300.0	0
Plutonium-239	211100000.0	0
Plutonium-240	57380000.0	0
Plutonium-241	126100.0	0
Americium-241	3784000.0	0
Curium-242	3912.0	0
Curium-244	158600.0	0
Test-Nuclide	1000.0	0
Inert-Tracer	∞	∞
Sulphur-Dioxide-S	∞	100
Sulphate	∞	1000
Carbon	∞	1000
Particulate	∞	0
Tracer	∞	100

Table 5(cont.) Species half lives and R<sub>c</sub> values



## 10. REFERENCES

- Baer M & Nester K (1992) 'Parametrisation of trace gas dry deposition velocities for a regional mesoscale diffusion model' *Ann. Geophysicae*, **10**, 912-923
- Baldocchi D D, Hicks B B & Camara P (1987) 'A canopy stomatal resistance model for gaseous deposition to vegetated surface' *Atmos. Environ.*, **21**, 91-101
- Brost R A, Wyngaard J C & Lenschow D H (1982) 'Marine stratocumulus layers> Part II: Turbulence budgets' *J. Atmos. Sc.* **39**, 818-836.
- Erismann J W (1994) 'Evaluation of a surface resistance parametrisation of sulphur dioxide' *Atmospheric Environment*, **28**, 2583-2594
- Erismann J W & Baldocchi D (1994) 'Modelling dry deposition of SO<sub>2</sub>' *Tellus*, **46B**, 159-171
- Erismann J W, Pul A V & Wyers P (1994) 'Parametrisation of surface resistance for the quantification of atmospheric deposition of acidifying pollutants and ozone' *Atmos. Environ.*, **28**, 2595-2607
- Grant A L M (1992) 'The structure of turbulence in the near-neutral atmospheric boundary layer' *J. Atmos. Sc.* **49**, 226-239.
- Hanna, S.R. (1982) 'Applications in air pollution modelling. In: Atmospheric Turbulence and Air Pollution Modelling' Ed.F.T.M. Nieuwstadt and H. van Dop, D Reidel Publishing Company, Dordrecht, Holland.
- Hibberd, M.F. and Sawford, B.L. (1994) 'A saline laboratory model of the planetary convective boundary layer' *Boundary-Layer Met.*, **69**, 229-250.
- Hudson, B. and Thomson, D.J. (1994) 'Dispersion in convective and neutral boundary layers using a random walk model' Met O (APR) Turbulence and Diffusion Note No. 210.
- Hurley, P.J. and Physick, W.L.(1993) 'A skewed homogeneous Lagrangian particle model for convective conditions' *Atmospheric Environment*, **27A**, No. 4, 619-624.
- Kitchen K P (1993) 'Nuclear Accident Response Model Program Documentation, Version 2' MetO(APR) Internal Technical Memorandum No.21
- Kitchen K P, Ryall D B & Maryon R H (1995) 'NAME II - Program documentation' Met O(APR) Internal Technical Memorandum No. 27
- Luhar, A.K. and Britter, R.E (1989) 'A random walk model for dispersion in inhomogeneous turbulence in a convective boundary layer' *Atmospheric Environment*, **23**, 1911-1924.
- Maryon R H (1993) 'Supplementary Notes on the Structure and Parametrization of NAME, Version 2' MetO(APR) Internal Technical Memorandum No.21



Maryon R H & M J Best 'NAME, ATMES and the boundary layer problem' Internal Met Office report: Met O(APR) TDN No. 204

Maryon, R.H. and Buckland, A.T. (1994) 'Diffusion in a Lagrangian multiple particle model: a sensitivity study' *Atmos. Environ.*, **28**, 2019-2038.

Maryon R H & Buckland A T 'Tropospheric dispersion: the first ten days after a puff release'. (In preparation).

Maryon R H, Ryall D B & Kitchen K P (1995) 'NAME II: A users guide to the UK Nuclear Accident Response Model' Met O(APR) Internal Technical Memorandum No. 28

Maryon R H, Smith F B, Conway B J & Goddard D M (1991) 'The UK Nuclear Accident Model', *Progress in Nuclear Energy*, **26**, No. 2, 85-104

Physick, W.L. and Hurley, P.J. (1993) 'A fast Lagrangian particle model for use with three-dimensional mesoscale models' *XXth International Technical Meeting on Air Pollution Modelling and its Application, Valencia, December 1993*.

Physick, W L. and Maryon, R.H. (1995) 'Near-source turbulence parametrization in the NAME model' Met O(APR) TDN No. 218.

Randerson, D (Ed.) (1984) 'Atmospheric science and power production', Washington, US Department of Energy, Office of Energy Research.

Sehmel, G.A. (1980) 'Particle and dry deposition: a review' *Atmos. Environ.*, **14**, 983-1011

Seinfeld, J.H. (1986) 'Atmospheric chemistry and physics of air pollution', New York, John Wiley and Sons.

Thomson, D.J. (1984) 'Random walk modelling of diffusion in inhomogeneous turbulence' *Q. Jl. R. Met. Soc.*, **110**, 1107-1120.

Thomson, D.J. (1987) 'Criteria for the selection of stochastic models of particle trajectories in turbulent flows' *J. Fluid Mech.*, **180**, 529-556.

Venkatram, A and Wyngaard, J.C. (Eds.) (1988) *Lectures on Air Pollution Modeling*, American Meteorological Society, Boston.

Walcek C J, Brost RA & Chang J S (1986) 'SO<sub>2</sub>, sulphate and HNO<sub>3</sub> deposition Velocities computed using regional landuse and meteorological data' *Atmos. Environ.*, **20**, 949-964.

Wilson, J.D., Legg, B.J. and Thomson, D.J. (1983) 'Calculation of particle trajectories in the presence of a gradient in turbulent-velocity variance' *Boundary-Layer Met.*, **27**, 163-169.



## Global Grid and Topography

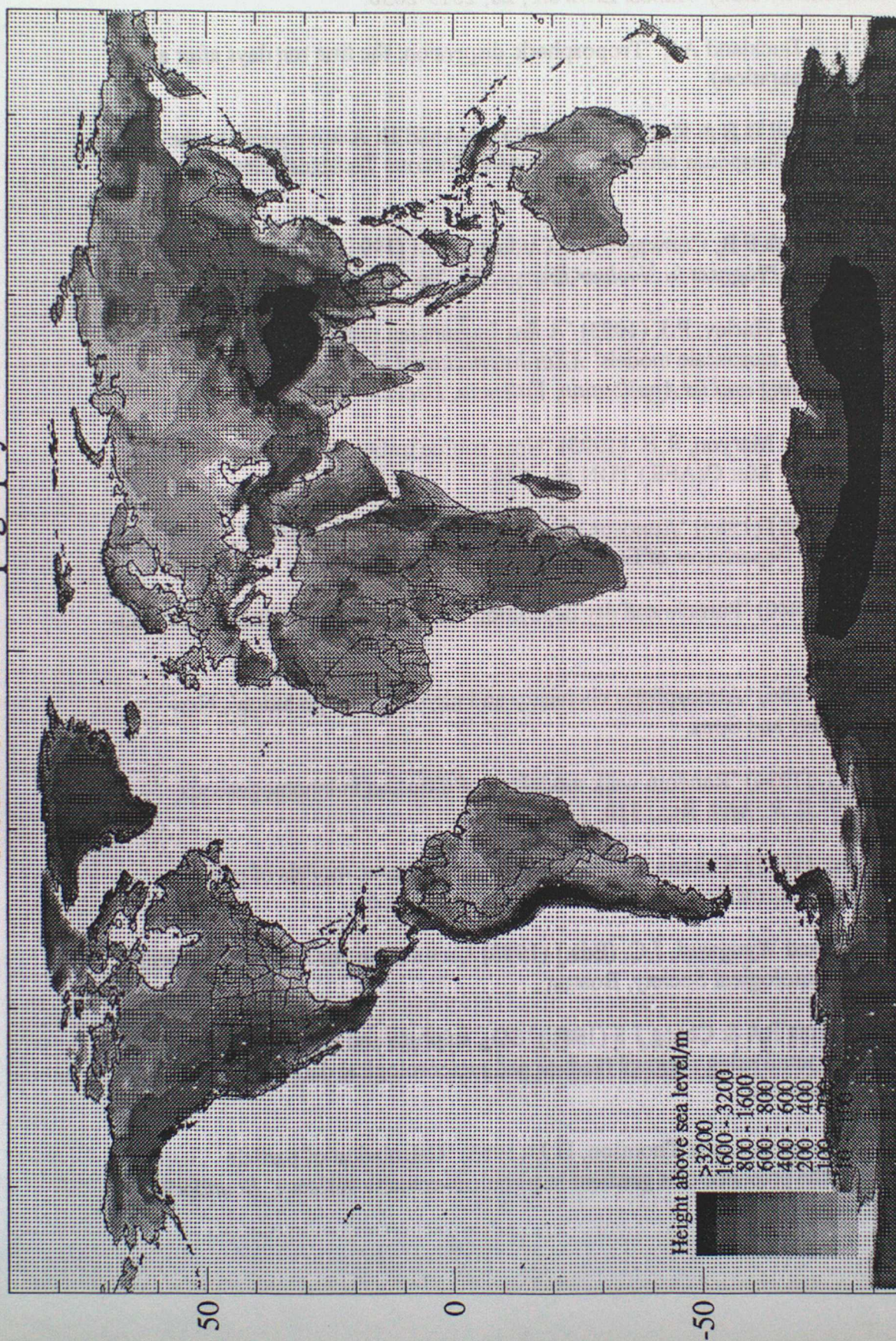


Figure 1 Global grid and topography



# Regional Area Grid and Topography

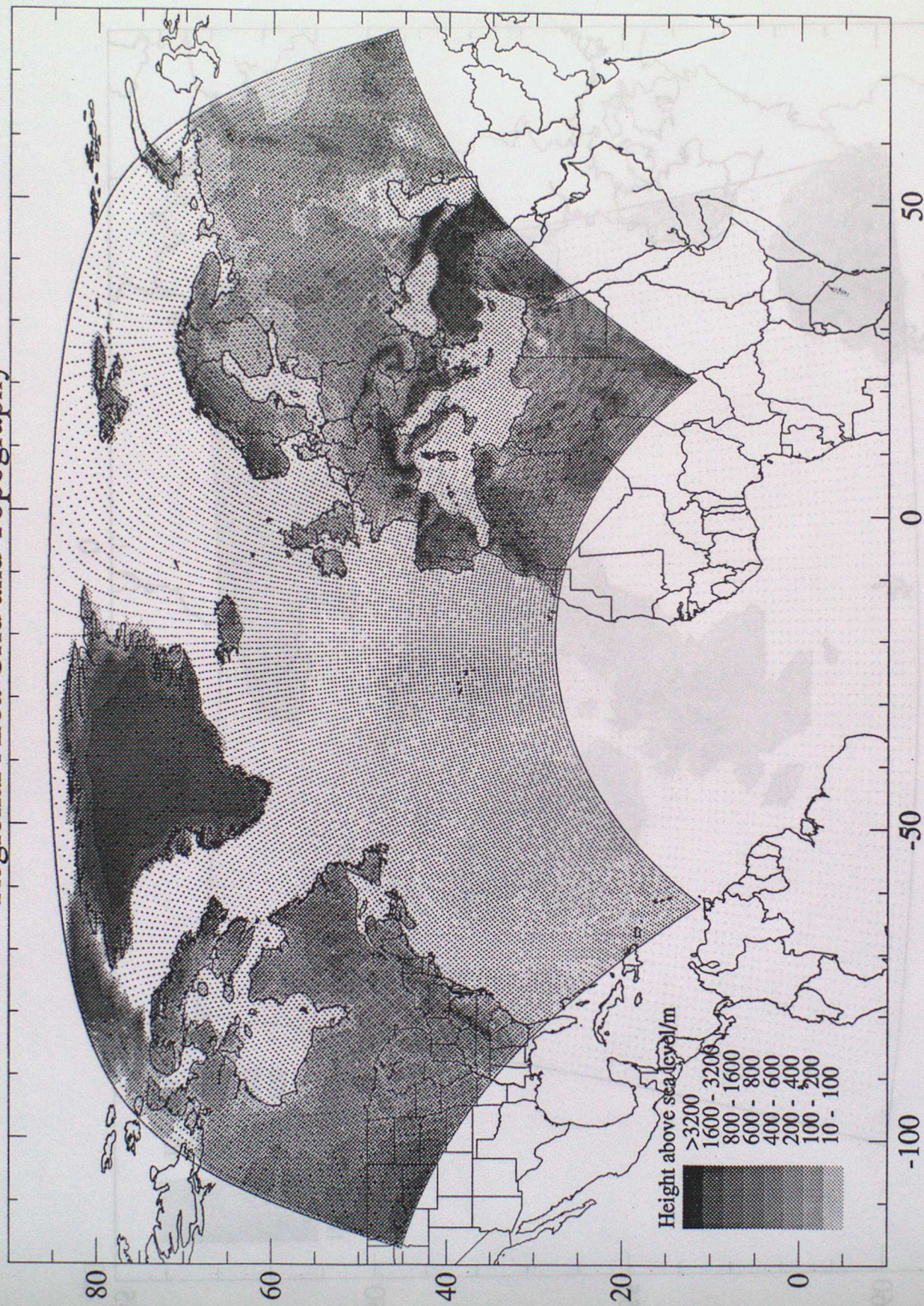


Figure 2 Regional grid and topography



# Mesoscale Area Grid and Topography

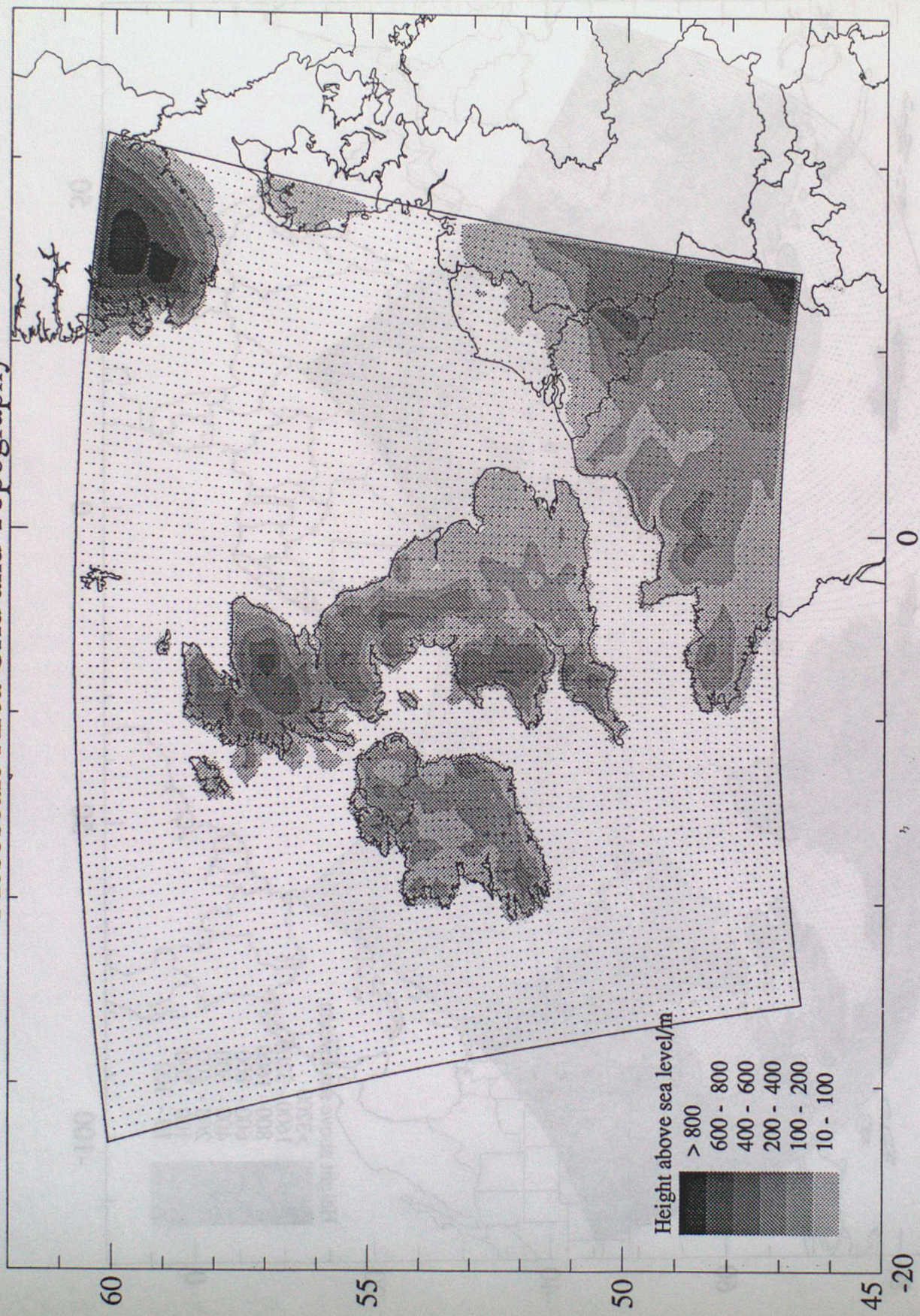


Figure 3 Mesoscale grid and topography



# High Resolution Rainfall grid and Topography

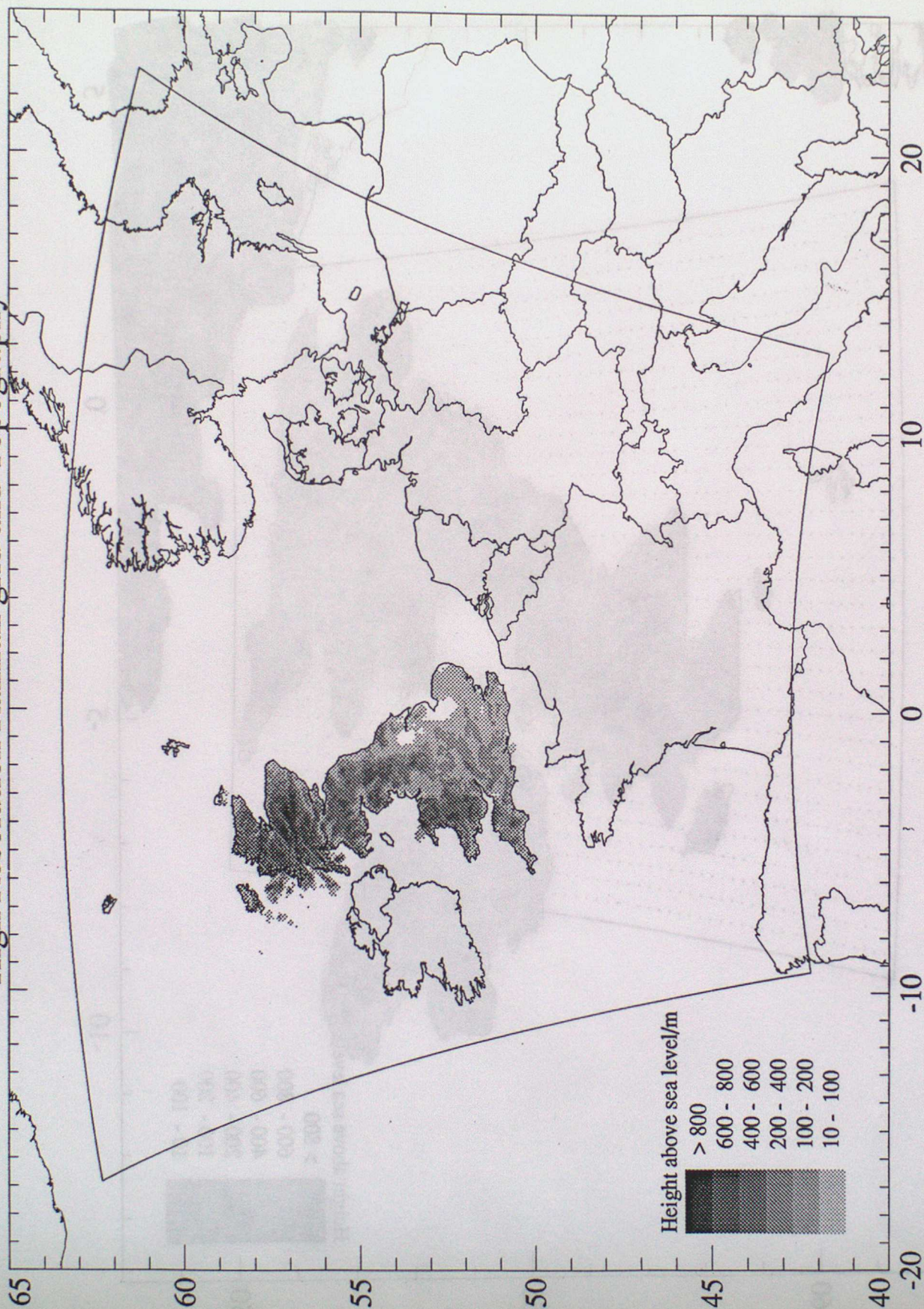


Figure 4 High Resolution Rainfall grid area and topography



# National Grid and Mesoscale Topography

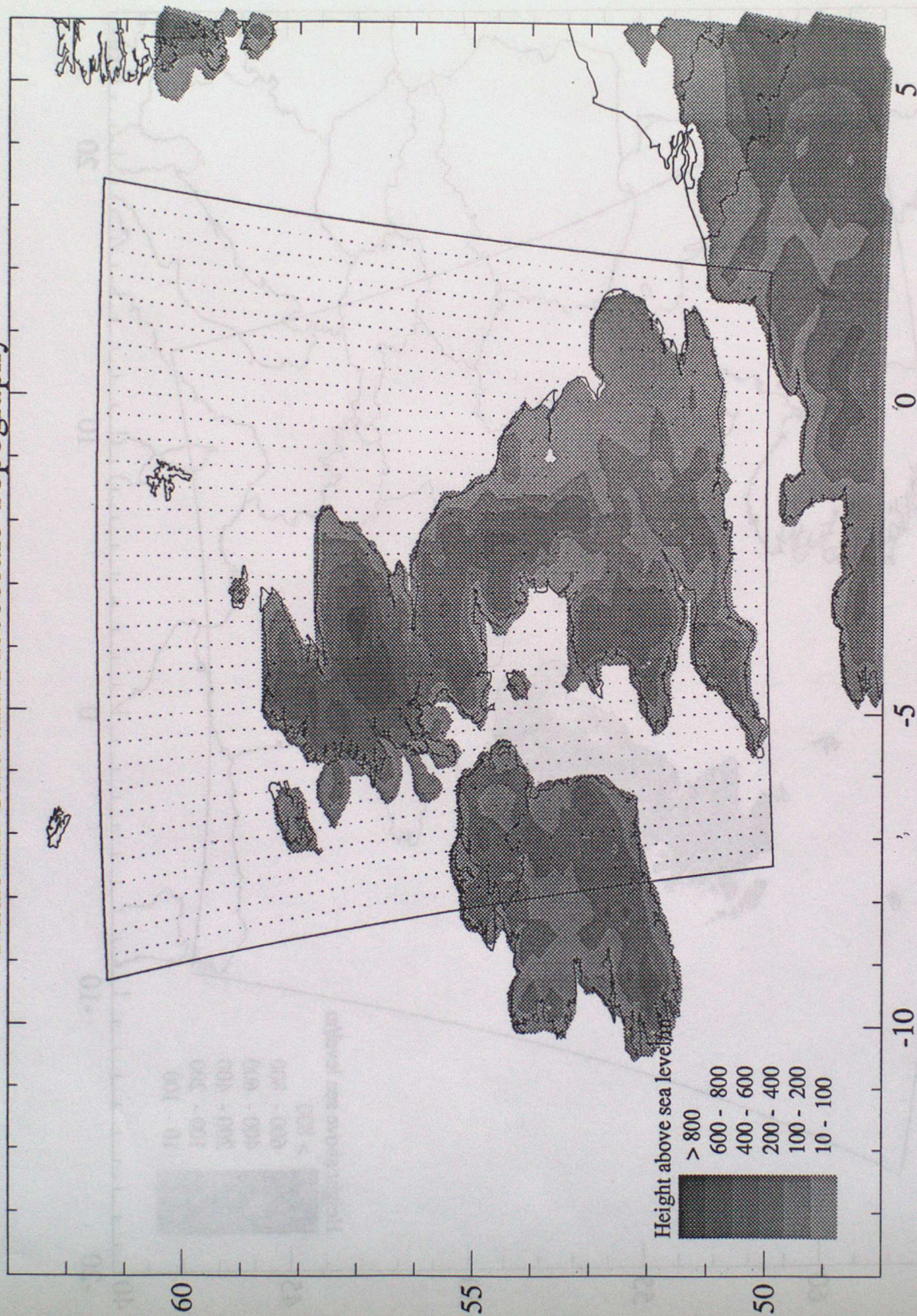


Figure 5 National grid (mesoscale topography shown)



# NAME II Structure

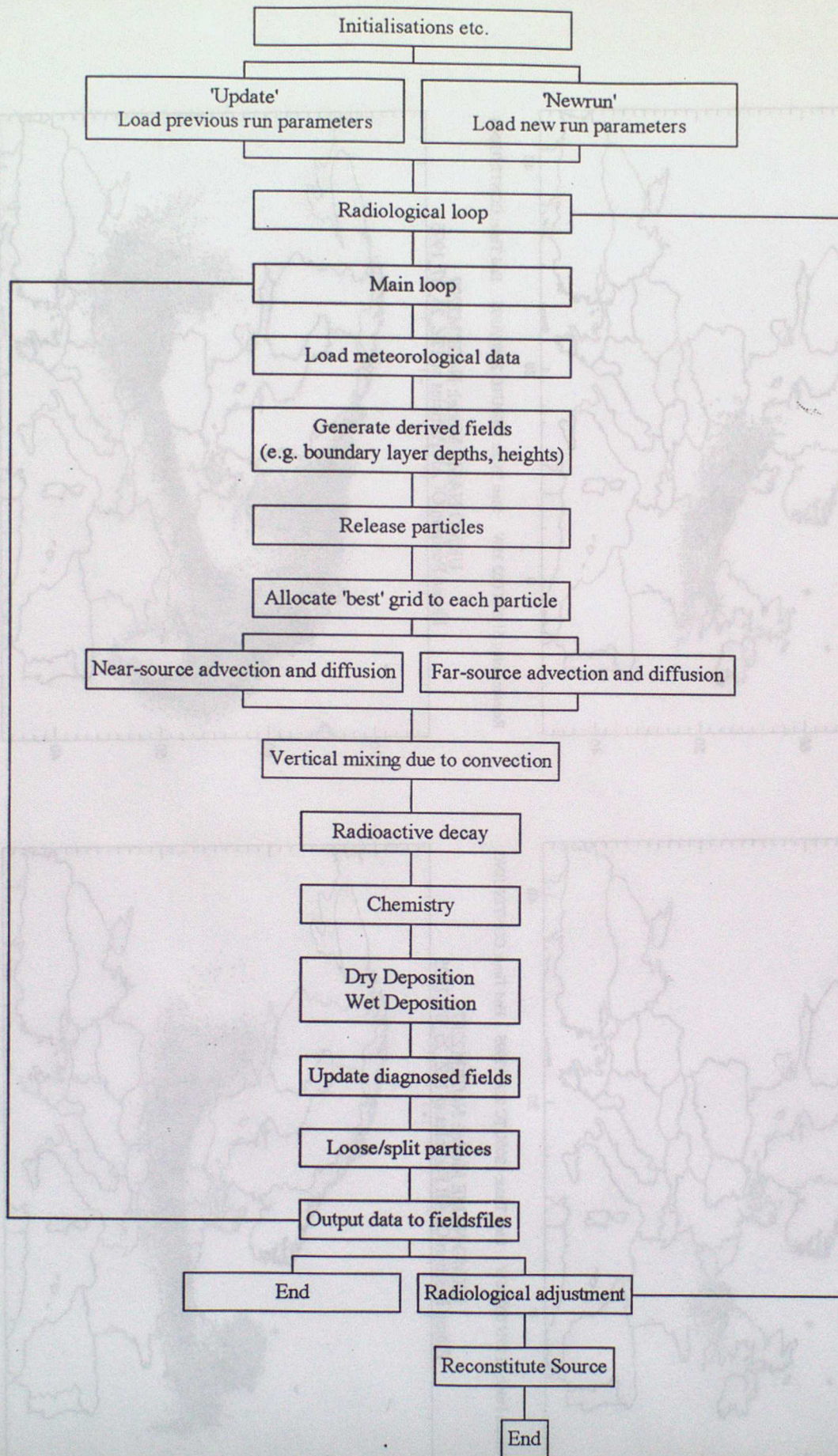
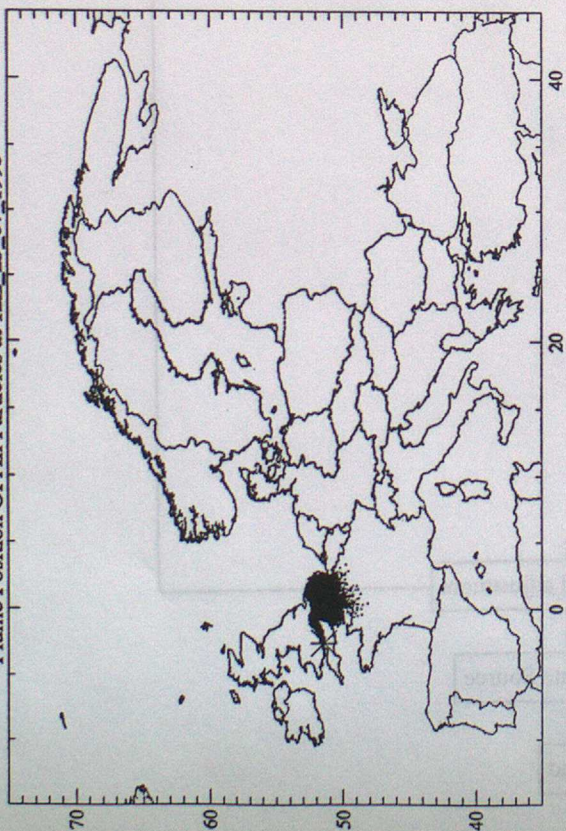


Figure 6 Illustration of NAME model structure

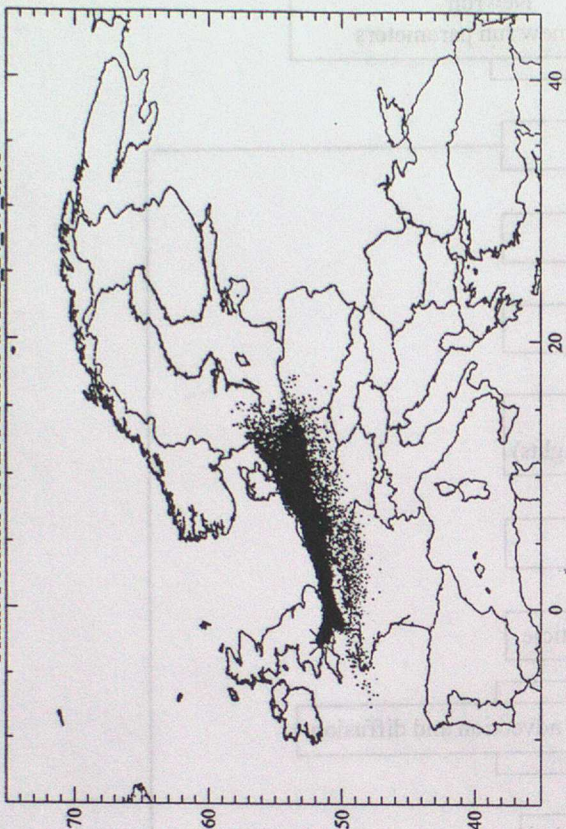


UKMO NAME Model: N4GRM2207  
Plume Position Of All Particles at 12Z\_23\_07\_1995



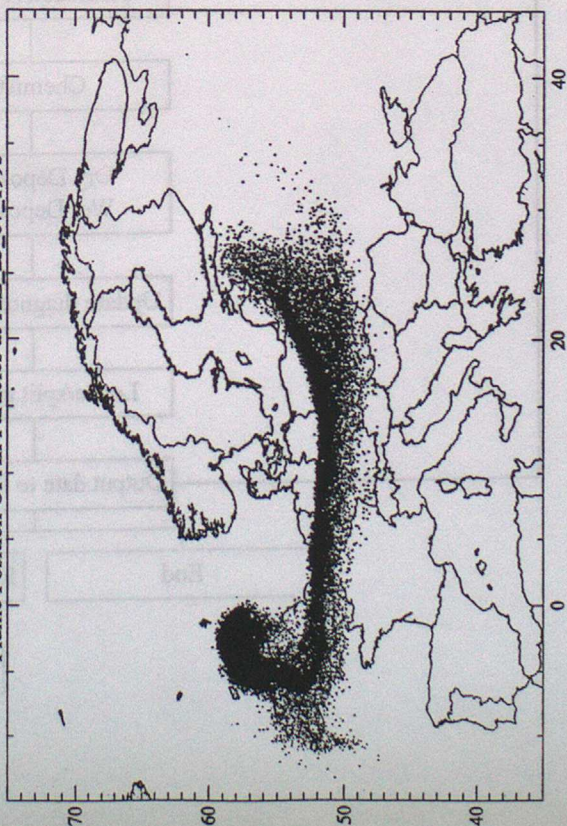
Release Point: 51 27N 002 35W Start Time: 1200UTC 22/07/1995 End Time: CONTINUING

UKMO NAME Model: N4GRM2207  
Plume Position Of All Particles at 12Z\_24\_07\_1995



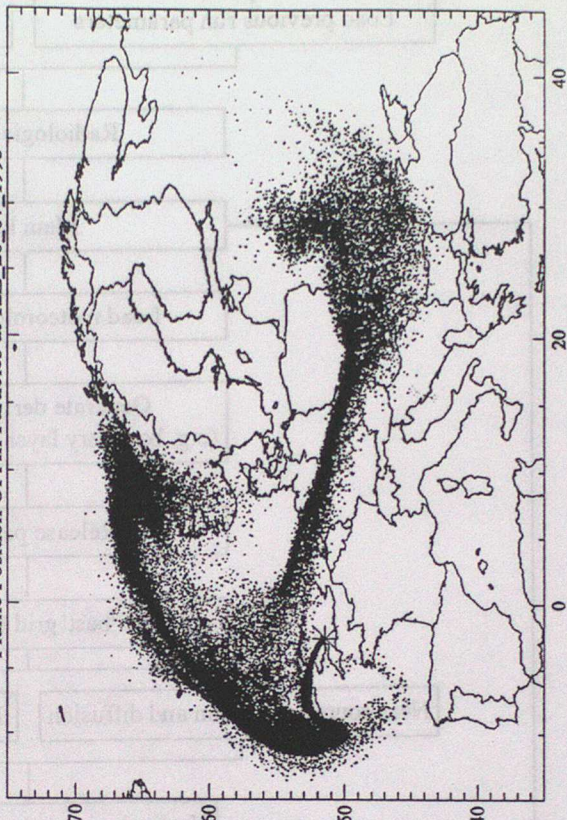
Release Point: 51 27N 002 35W Start Time: 1200UTC 22/07/1995 End Time: CONTINUING

UKMO NAME Model: N4GRM2207  
Plume Position Of All Particles at 12Z\_25\_07\_1995



Release Point: 51 27N 002 35W Start Time: 1200UTC 22/07/1995 End Time: CONTINUING

UKMO NAME Model: N4GRM2207  
Plume Position Of All Particles at 12Z\_26\_07\_1995



Release Point: 51 27N 002 35W Start Time: 1200UTC 22/07/1995 End Time: CONTINUING

Figure 7 Particle positions 24, 48, 72 & 96 hours after release



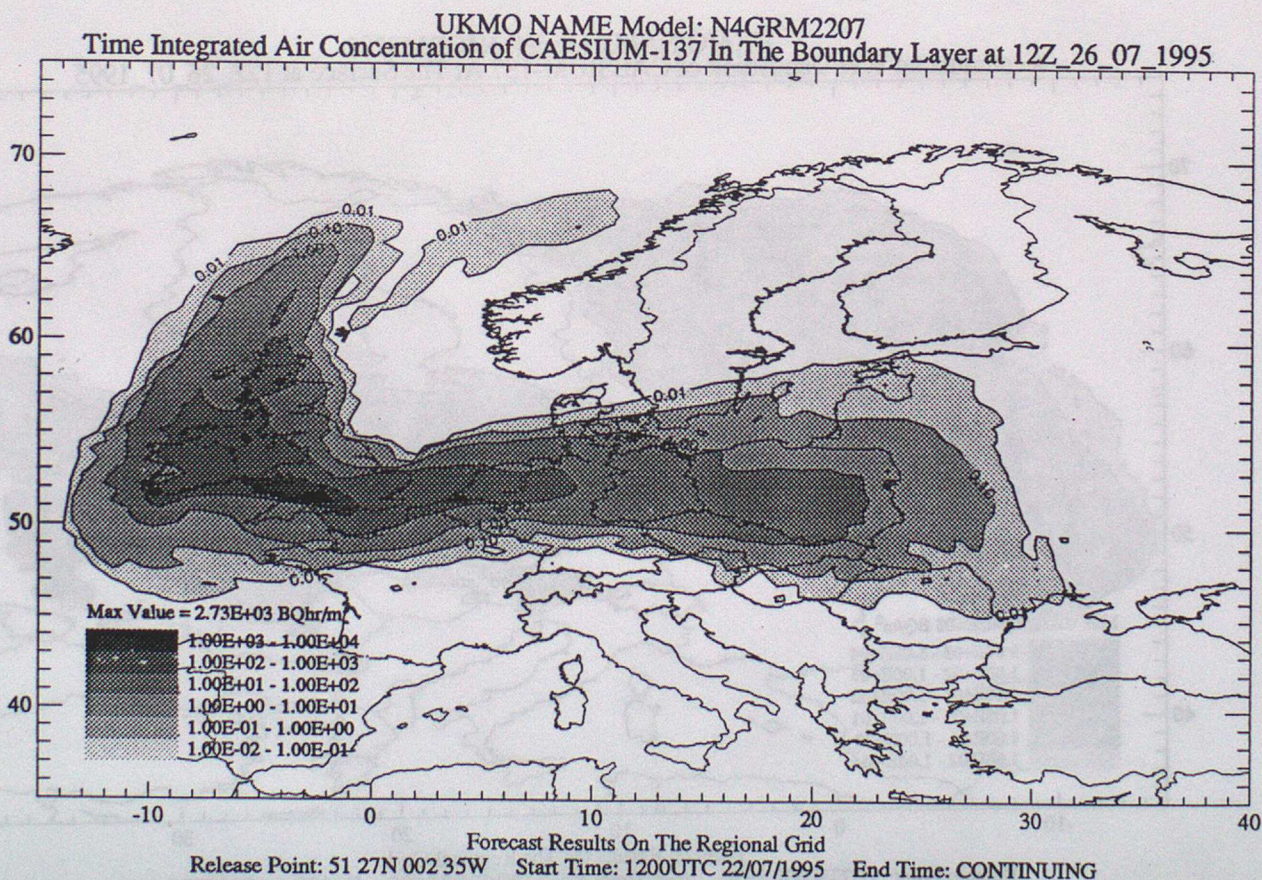
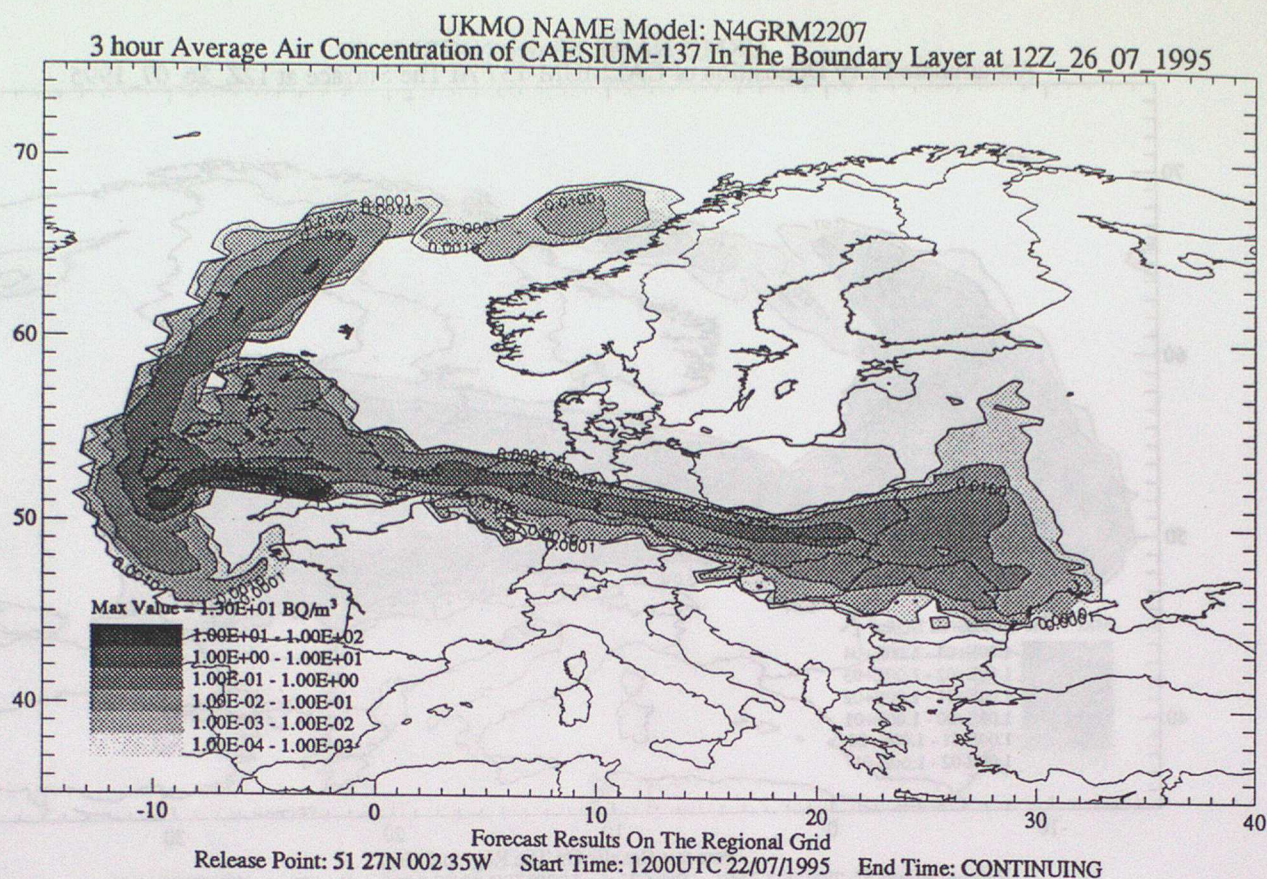
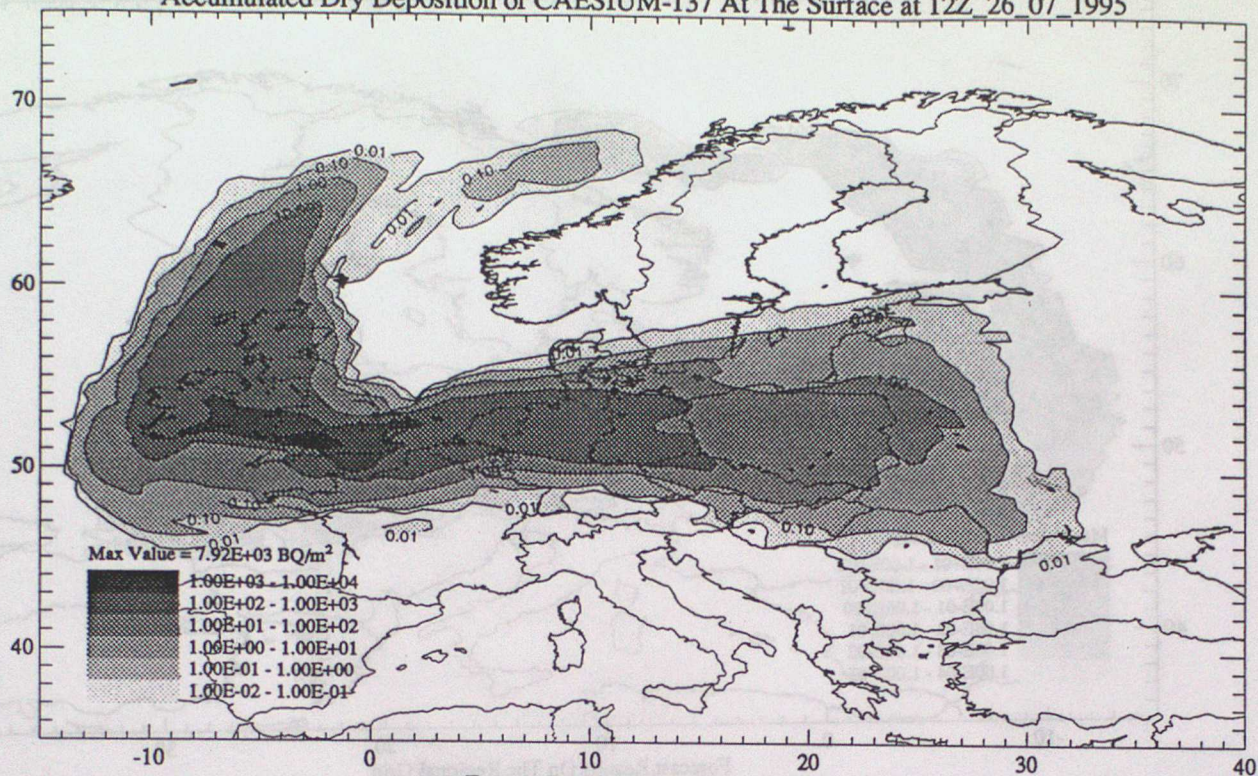


Figure 8 3 hour averaged and time integrated air concentrations at T+96

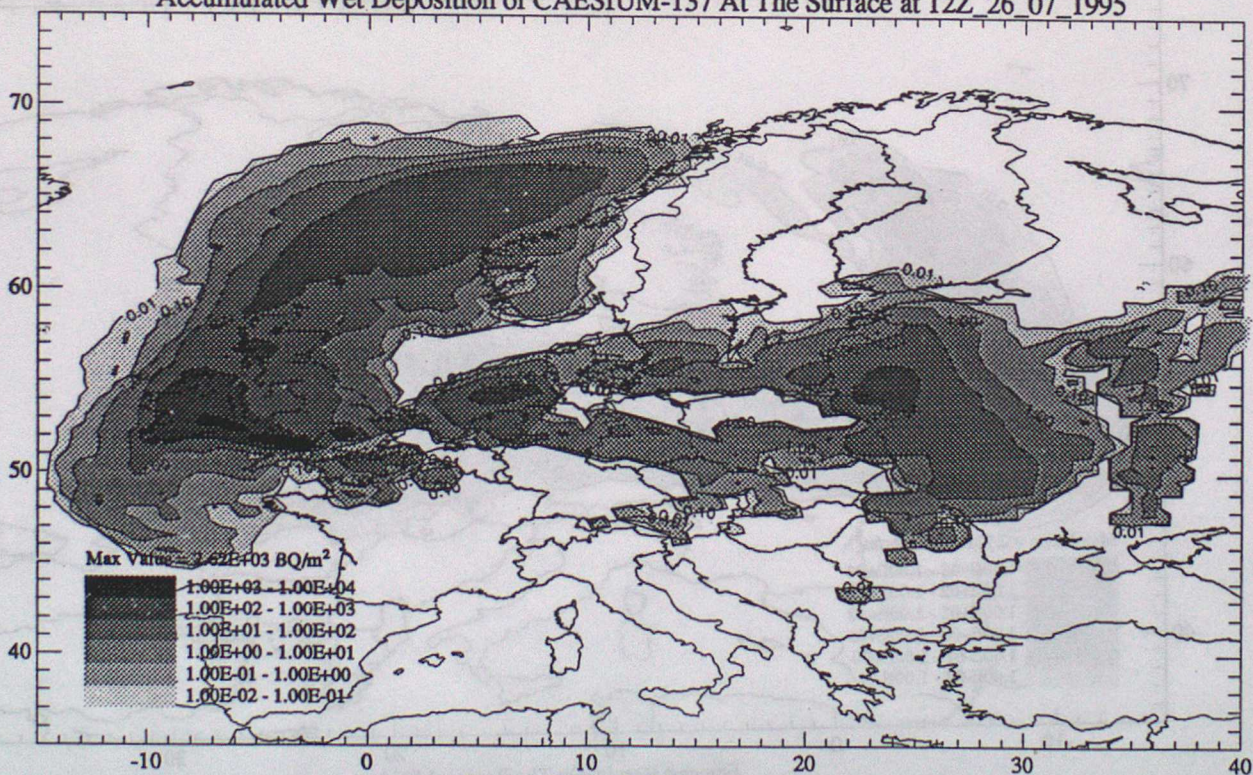


UKMO NAME Model: N4GRM2207  
Accumulated Dry Deposition of CAESIUM-137 At The Surface at 12Z 26 07 1995



Forecast Results On The Regional Grid  
Release Point: 51 27N 002 35W Start Time: 1200UTC 22/07/1995 End Time: CONTINUING

UKMO NAME Model: N4GRM2207  
Accumulated Wet Deposition of CAESIUM-137 At The Surface at 12Z 26 07 1995

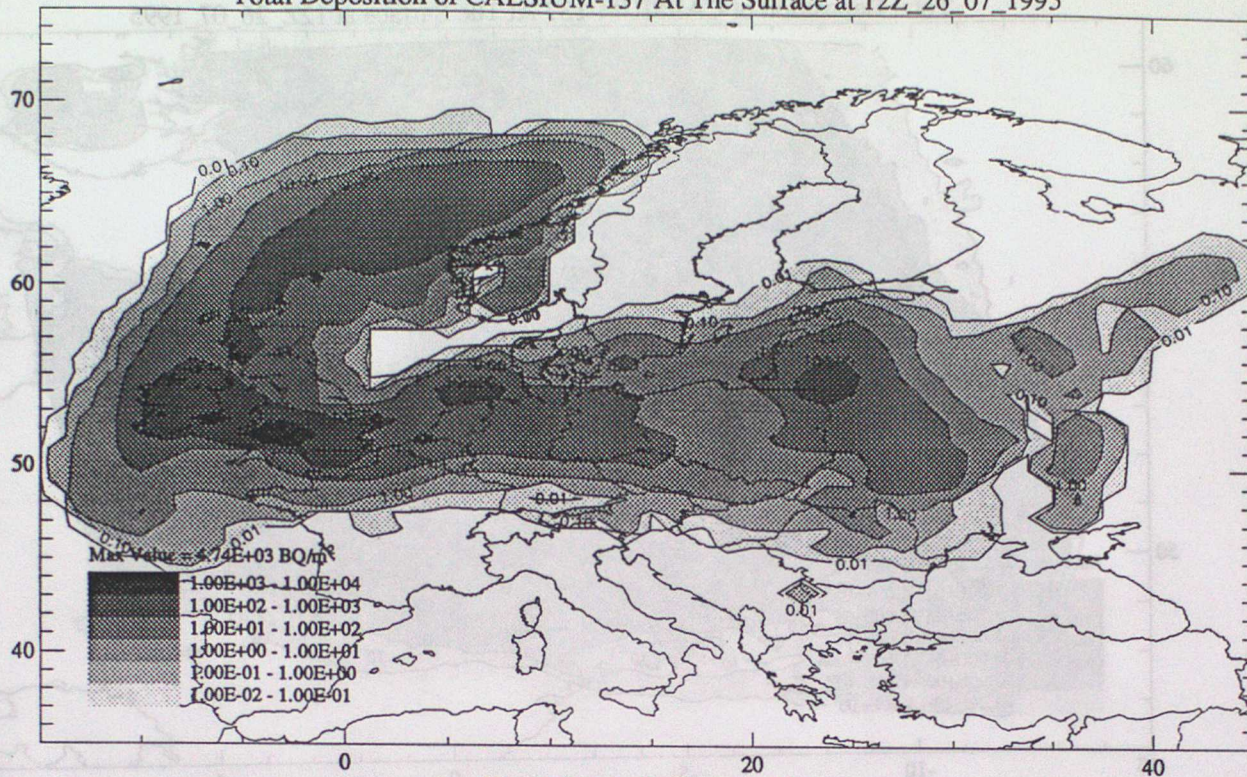


Forecast Results On The Regional Grid  
Release Point: 51 27N 002 35W Start Time: 1200UTC 22/07/1995 End Time: CONTINUING

Figure 9 Accumulated dry and wet depositions at T+96

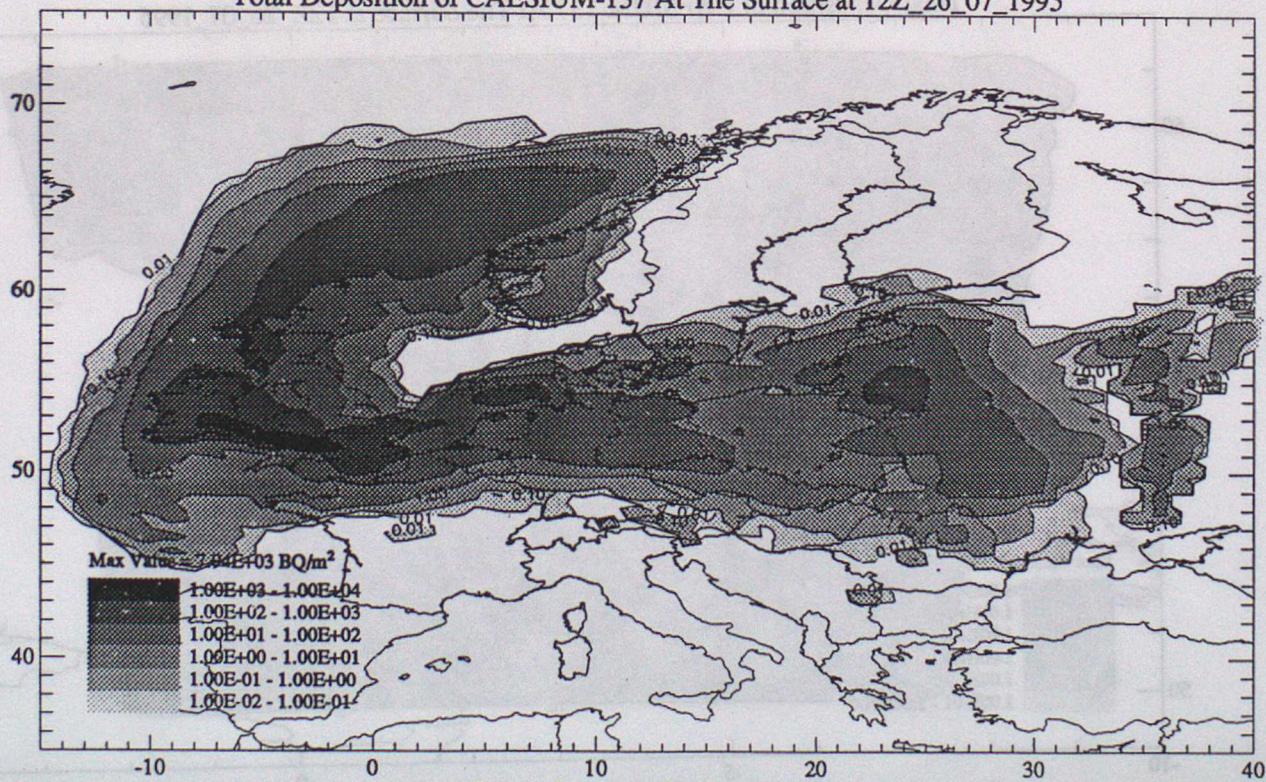


UKMO NAME Model: N4GRM2207  
Total Deposition of CAESIUM-137 At The Surface at 12Z, 26\_07\_1995



Forecast Results On The Global Grid  
Release Point: 51 27N 002 35W Start Time: 1200UTC 22/07/1995 End Time: CONTINUING

UKMO NAME Model: N4GRM2207  
Total Deposition of CAESIUM-137 At The Surface at 12Z, 26\_07\_1995

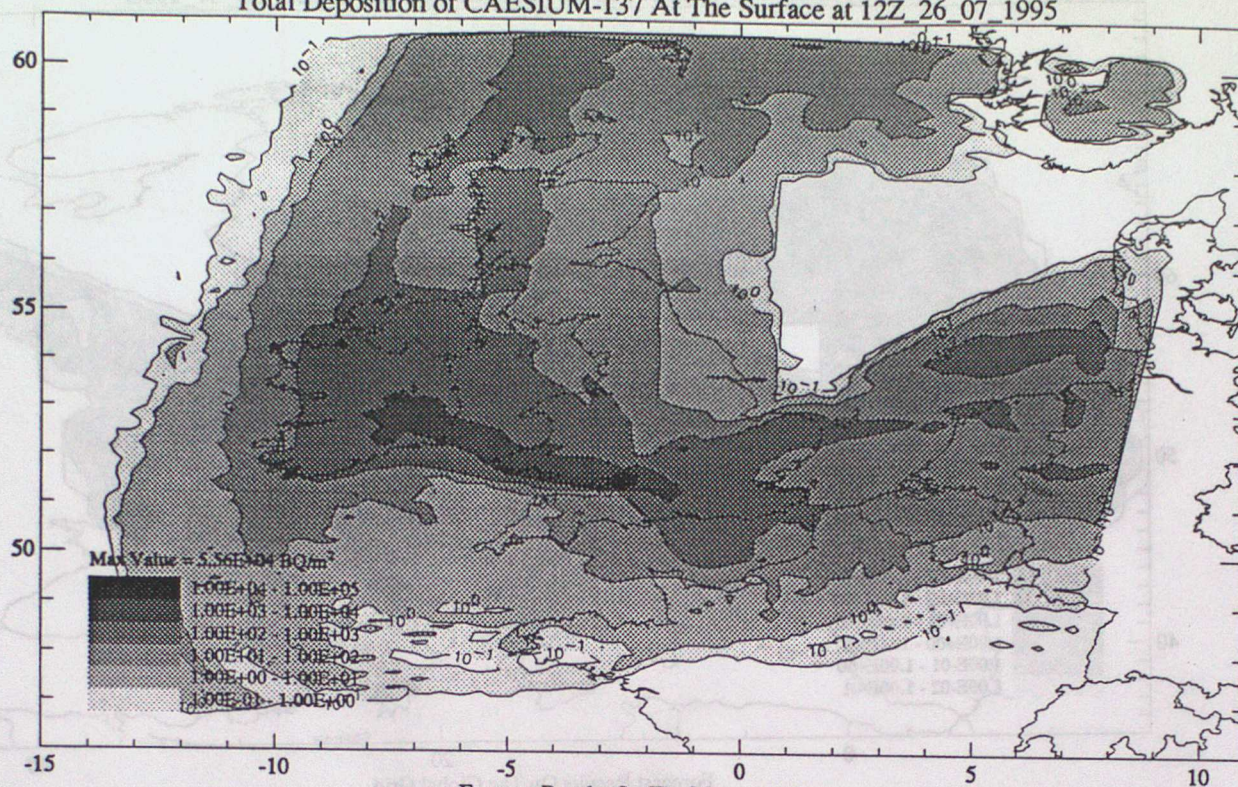


Forecast Results On The Regional Grid  
Release Point: 51 27N 002 35W Start Time: 1200UTC 22/07/1995 End Time: CONTINUING

Figure 10 Total deposition at T+96 analysed on the global and regional grids

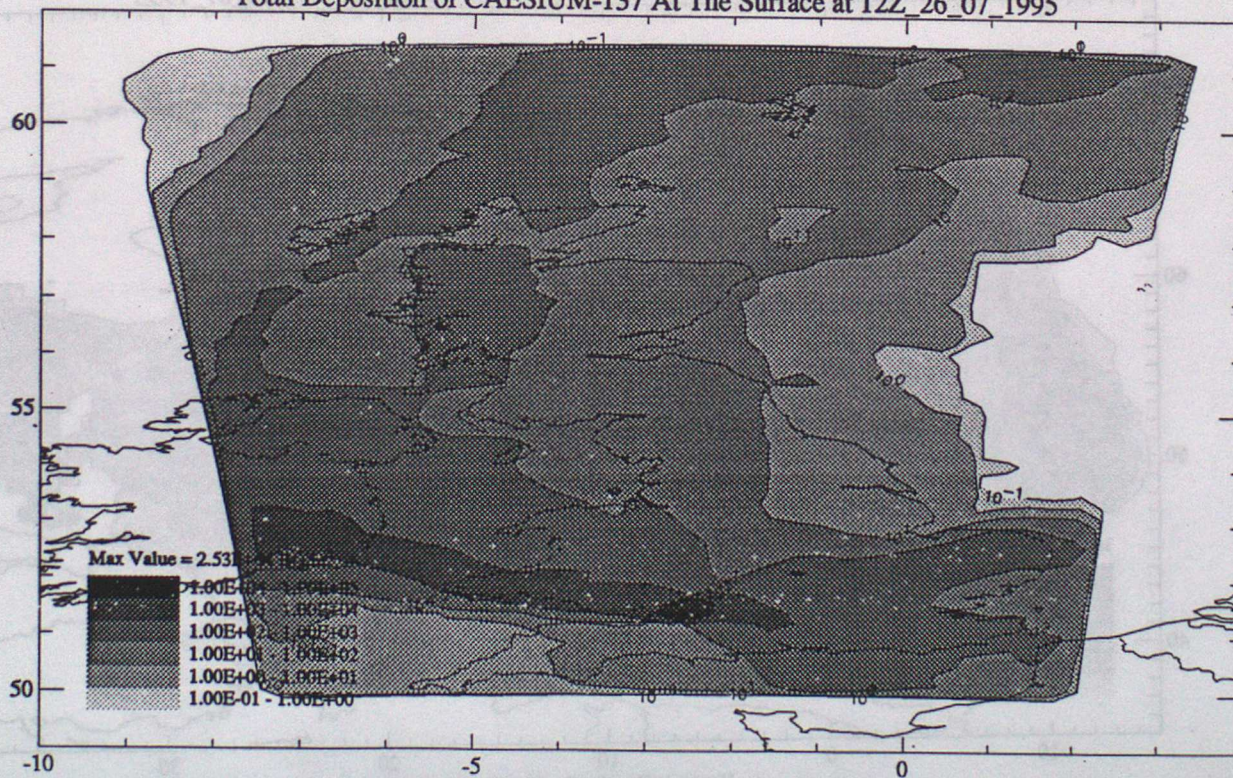


UKMO NAME Model: N4GRM2207  
Total Deposition of CAESIUM-137 At The Surface at 12Z, 26\_07\_1995



Forecast Results On The Mesoscale Grid  
Release Point: 51 27N 002 35W Start Time: 1200UTC 22/07/1995 End Time: CONTINUING

UKMO NAME Model: N4GRM2207  
Total Deposition of CAESIUM-137 At The Surface at 12Z, 26\_07\_1995

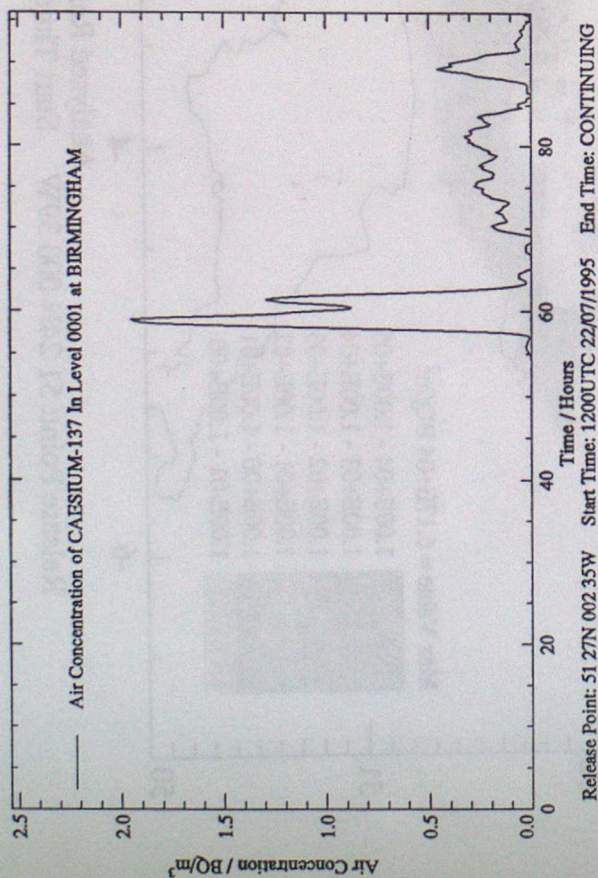


Forecast Results On The National Grid Grid  
Release Point: 51 27N 002 35W Start Time: 1200UTC 22/07/1995 End Time: CONTINUING

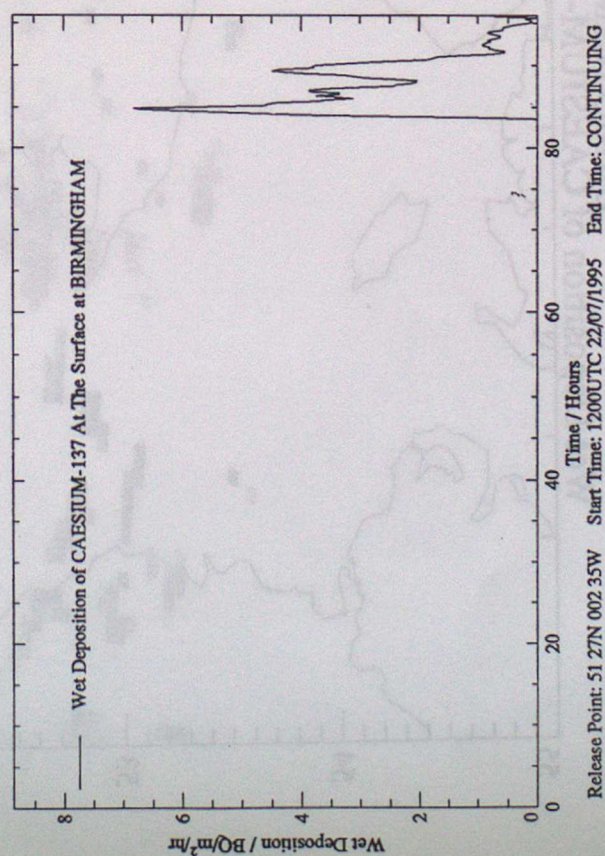
Figure 11 Total deposition at T+96 analysed on the mesoscale and national grids



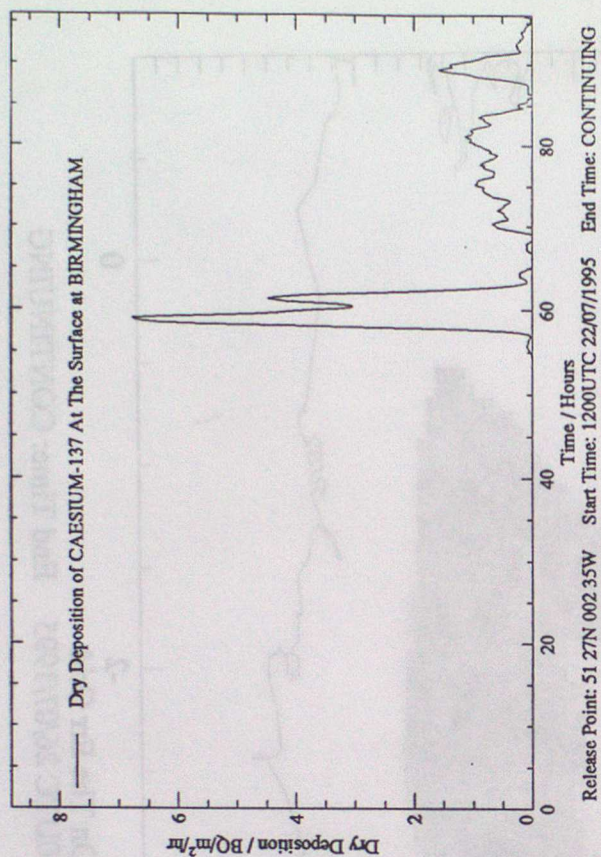
UKMO NAME Model: N4GRM2207



UKMO NAME Model: N4GRM2207



UKMO NAME Model: N4GRM2207



UKMO NAME Model: N4GRM2207

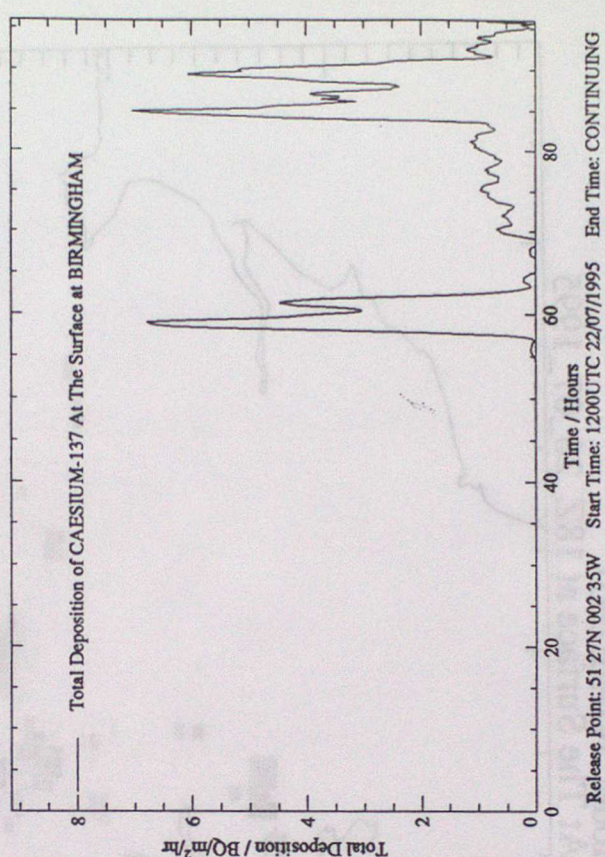
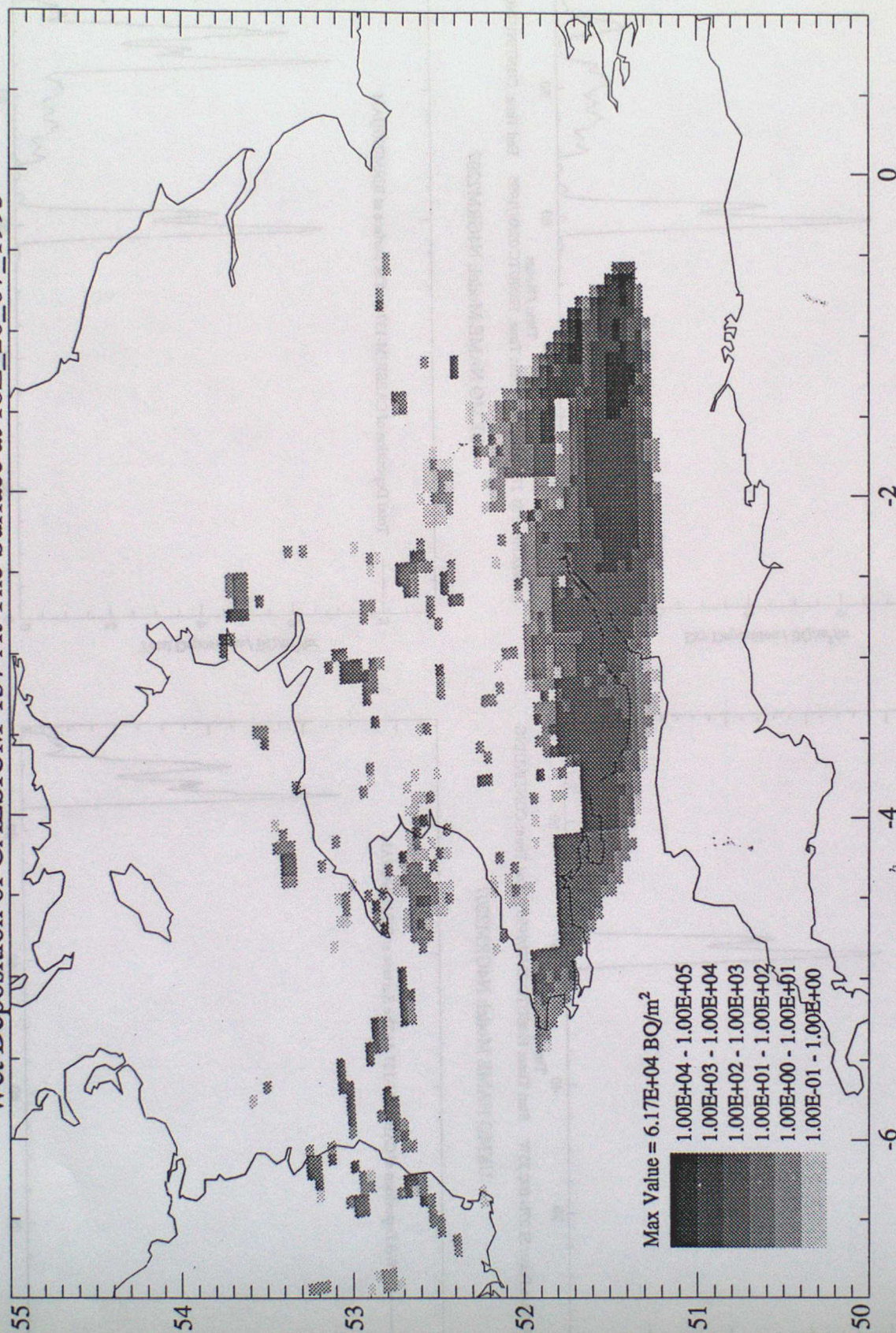


Figure 12 Time series traces for Birmingham



# UKMO NAME Model: N1ME2607 Wet Deposition of CAESIUM-137 At The Surface at 18Z\_26\_07\_1995



Release Point: 51 24N 000 39W    Start Time: 0600UTC 26/07/1995    End Time: CONTINUING

Figure 13 High resolution wet deposition field at T+12